PTEP

Prog. Theor. Exp. Phys. **2020**, 113B01 (39 pages)
DOI: 10.1093/ptep/ptaa112

Physics of parameter correlations around the solar-scale enhancement in neutrino theory with unitarity violation

Ivan Martinez-Soler[1,2,3,*] and Hisakazu Minakata[4,*]

[1]*Theoretical Physics Department, Fermi National Accelerator Laboratory, P.O. Box 500, Batavia IL 60510, USA*
[2]*Department of Physics and Astronomy, Northwestern University, Evanston, IL 60208, USA*
[3]*Colegio de Física Fundamental e Interdisciplinaria de las Américas (COFI), 254 Norzagaray street, San Juan, Puerto Rico 00901*
[4]*Center for Neutrino Physics, Department of Physics, Virginia Tech, Blacksburg, Virginia 24061, USA*
E-mail: ivan.martinezsoler@northwestern.edu, minakata71@vt.edu

Received May 18, 2020; Revised July 7, 2020; Accepted July 7, 2020; Published November 2, 2020

We discuss the physics of the three neutrino flavor transformation with non-unitary mixing matrix, with particular attention to the correlation between the νSM- and the α parameters which represent the effect of unitarity-violating (UV) new physics. Towards this goal, a new perturbative framework is created to illuminate the effect of non-unitarity in the region of the solar-scale enhanced oscillations. We refute the skepticism about the physical reality of the νStandard Model CP phase δ–α parameter phase correlation by analysis with the SOL convention of $U_{\rm MNS}$, in which $e^{\pm i\delta}$ is attached to s_{12}. Then, a comparative study between the solar- and atmospheric-scale oscillation regions allowed by the framework reveals a dynamical δ–(blobs of the α parameters) correlation in the solar oscillation region, in sharp contrast to the "chiral"-type phase correlation $[e^{-i\delta}\bar{\alpha}_{\mu e},\ e^{-i\delta}\bar{\alpha}_{\tau e},\ \bar{\alpha}_{\tau\mu}]$ in the Particle Data Group convention seen in the atmospheric oscillation region. An explicit perturbative calculation to the first order in the $\nu_\mu \to \nu_e$ channel allows us to decompose the UV related part of the probability into the unitary evolution part and the genuine non-unitary part. We observe that the effect of non-unitarity tends to cancel between these two parts, as well as between the different $\alpha_{\beta\gamma}$ parameters.

Subject Index B54

1. Introduction

The discovery of neutrino oscillation and hence neutrino mass [1,2] under the framework of three-generation lepton flavor mixing [3] created a new field of research in particle physics. It led to the construction of the next-generation accelerator and underground experiments with the massive detectors Hyper-Kamiokande [4] and DUNE [5]. These projects are going to establish CP violation due to the lepton Kobayashi–Maskawa (KM) phase [6], possible lepton counterpart of the quark CP violation [7]. They will also determine the neutrino mass ordering at high confidence level by utilizing the Earth matter effect [8,9]. Of course, the flagship projects will be challenged by the ongoing [10–12] and the other upcoming experiments, for example, ESSνSB [13], JUNO [14], T2KK [15],[1] INO [17], IceCube-Gen2/PINGU [18] and KM3NeT/ORCA [19], which compete for the same goals.

[1] A possible acronym used in Ref. [16], but now for the updated name for the setting, "Tokai-to-Kamioka observatory-Korea neutrino observatory".

Funded by SCOAP[3]

Toward establishing the three-flavor mixing scheme, in particular in the absence of a confirmed anomaly beyond the neutrino-mass embedded Standard Model (νSM), one of the most important topics in the future would be the high-precision paradigm test.[2] In this context, leptonic unitarity tests, either by closing the unitarity triangle [21], or by an alternative method of constraining the models of unitarity violation (UV) at high-energy [22,23] or low-energy scales [24–26], are extensively discussed.[3] The references in Refs. [27–35], for example, include the past and the subsequent development of the subjects. A summary of the current constraints on UV is given e.g., in Refs. [26,36].

It was observed that in the 3×3 active neutrino subspace the evolution of the system can be formulated on the same footing in low-scale as well as high-scale UV scenarios [25,26]. Nonetheless, dynamics of the three neutrino system with non-unitary mixing in matter has not been investigated in sufficient depth. Apart from numerically implemented calculation carried out in some of the aforementioned references, only a very limited effort was devoted to analytical understanding of the system so far. This is in sharp contrast to the fact that a great amount of effort was devoted to understanding the three-flavor neutrino oscillation.[4] A general result known to us so far is the exact S matrix with non-unitarity in matter with constant density [25] calculated by using the Kimura-Takamura-Yokomakura-type construction [37]. It allows us to obtain the exact expression of the oscillation probability with non-unitarity.

In a previous paper [38], we started a systematic investigation of the analytic structure of the three-neutrino evolution in matter with non-unitarity. We have used the so-called α parametrization [23] to implement non-unitarity in the three-neutrino system. Under the Particle Data Group (PDG) convention $U_{\rm PDG}$ [39] of the flavor-mixing matrix $U_{\rm MNS}$, it parametrizes the 3×3 non-unitary mixing matrix N as

$$N = \left\{ \mathbf{1} - \begin{bmatrix} \bar{\alpha}_{ee} & 0 & 0 \\ \bar{\alpha}_{\mu e} & \bar{\alpha}_{\mu\mu} & 0 \\ \bar{\alpha}_{\tau e} & \bar{\alpha}_{\tau\mu} & \bar{\alpha}_{\tau\tau} \end{bmatrix} \right\} U_{\rm PDG}. \tag{1}$$

Using a perturbative framework dubbed as the "helio-UV perturbation theory" (a UV-extended version of [40]) with two kinds of expansion parameters, the helio-to-terrestial ratio $\epsilon \approx \Delta m^2_{21}/\Delta m^2_{31}$ and the α parameters, we computed the oscillation probability valid to the first-order in the expansion parameters. The region of validity of the perturbative framework spans the one around the atmospheric-scale enhanced oscillations which cover the relevant region for the ongoing and the next-generation long-baseline (LBL) accelerator neutrino oscillation experiments. The possibility of application to the data from the near-future facilities and the currently almost non-understood properties of the system may justify the examination even though it is to the first order in expansion.

In our view, the most significant observation in Ref. [38] is that the νSM CP phase δ and the complex α parameters defined above have an intriguing phase correlation of the form $[e^{-i\delta}\bar{\alpha}_{\mu e}, e^{-i\delta}\bar{\alpha}_{\tau e}, \bar{\alpha}_{\tau\mu}]$. What is unique in the phase correlation is that it universally holds in all the oscillation channels as well as unitary and non-unitary parts of the oscillation probability. One should note that the definition

[2] For possible candidates of the anomalies which suggest physics beyond the νSM see e.g. Ref. [20].

[3] It is appropriate to mention that in the physics literature "UV" usually means "ultraviolet". However, in this paper "UV" is used as an abbreviation for "unitarity violation" or "unitarity-violating".

[4] Here, we give a cautious remark that when the term "neutrino oscillation" is used in this paper, or often in many other literatures, it may imply not only the original meaning, but also something beyond, such as "neutrino flavor transformation", or "neutrino flavor conversion", depending upon the context.

of the α parameters, and consequently the precise form of the correlation between the CP phases, depends on the phase convention of the lepton flavor mixing Maki-Nakagawa-Sakata (MNS) matrix; see Sect. 4.1.[5]

A puzzling feature of the δ–α parameter phase correlation in Ref. [38] is that it disappears in the SOL convention of $U_{\rm MNS}$ in which $e^{\pm i\delta}$ is attached to s_{12}. This triggered a skepticism of the nature of phase correlation, which may allow the following two alternative interpretations:

(1) Existence of the SOL phase convention of $U_{\rm MNS}$ in which δ and α phase correlation is absent implies that the CP phase correlation is not physical, but an artifact of an inadequate choice of $U_{\rm MNS}$ phase convention.
(2) Physics must be $U_{\rm MNS}$ convention independent. In all the other conventions of $U_{\rm MNS}$ except for the SOL, there exists δ–α parameter phase correlation. Therefore, the existence of phase correlation is generic and it must be physical.

If the interpretation (1) and the reasoning behind it are correct, δ and α phase correlation must be absent under the SOL convention of $U_{\rm MNS}$ everywhere in the allowed kinematical regions. Conversely, if we see a non-vanishing phase correlation in the oscillation probability calculated with the SOL convention somewhere, it implies that the interpretation (1) cannot be true. We will show throughout this paper that the interpretation (2) holds by investigation of the system in the region of the solar-scale enhanced oscillation.

2. The goal of this paper by itself, and in combining a companion work [38]

In this paper, we discuss the physics of neutrino flavor transformation in the region of solar-scale enhanced oscillation.[6] We will try to achieve the following two goals:

- To examine the system of the three-flavor neutrinos in the SOL convention ($e^{\pm i\delta}$ attached to s_{12}) of $U_{\rm MNS}$ in the region of the enhanced solar oscillation, which will testify to the physical reality of the correlation between the νSM–UV α parameter phases.
- To understand the νSM–UV parameter correlation in a more generic context and in the wider kinematical region by combining the results of this and previous works [38].

A few words on the examination of the "solar region" should be said. We feel that an immense need exists for the real understanding of parameter correlation in theories with non-unitarity, in particular outside the region investigated in Ref. [38]. The natural "field of research" for this purpose is the region of solar-scale enhanced oscillation, the unique place for enhancement other than the atmospheric one in our world of the three generation leptons. The feature can be seen clearly in the "terrestrial-friendly" region of the E vs. L plot, e.g., in Refs. [41,42]; the latter of those works also provides a brief summary of recent activities on atmospheric neutrinos at low energies. We note that the solar region has been the target of investigation for a long time, see e.g., Refs. [43–46] and

[5] In the ATM phase convention of $U_{\rm MNS}$ in which $e^{\pm i\delta}$ is attached to s_{23}, the phase correlation takes the form $[e^{-i\delta}\alpha_{\mu e}, \alpha_{\tau e}, e^{i\delta}\alpha_{\tau\mu}]$.

[6] The feature of merely replacing the atmospheric oscillation with the solar one may trigger the question "Are you attempting another experiment replacing copper with iron?". At this stage, we would like to say that a mere change in the field of exercise brings new insights to us because the system is so rich in dynamics, with the extra nine UV parameters introduced into the νSM system. In Sects. 6 and 7, the reader will see our clear-cut full answer to this question.

possibly others that we may have missed, mainly in the context of atmospheric neutrino observation at low energies. It should also be mentioned that this topic is now receiving renewed interest [41,42] given the new possibilities of gigantic detectors such as JUNO [47], DUNE [48], and Hyper-K [49]. Thus, the second goal of this paper is to achieve a deeper understanding of parameter correlation by combining knowledge in the regions of atmospheric-scale and the solar-scale enhanced oscillations.

Very recently, we have formulated a perturbative framework in the νSM, dubbed as the "solar resonance perturbation theory" [41], the validity of which is around the very region of our interest. We extend this perturbative framework to include the effect of UV, by treating the α parameters as the additional expansion parameters. Using this framework, we investigate dynamics of the three neutrino evolution with a non-unitary mixing matrix under the constant matter density approximation, with particular attention to the parameter correlation. We will show that the system displays a rich, new phenomenon of clustering of the νSM and the UV variables.

Nonetheless, we find it insufficient to rely on analytic treatment based on perturbation theory to extract the characteristic feature of the system due to a new and intricate feature of the parameter correlation. For this reason we rely also on exact numerical analyses as well as the perturbative formula we derive in this paper to elucidate the physics of the parameter correlation in the region of enhanced solar-scale oscillation. It will be particularly illuminating when our analysis is done in a style of comparative study between the solar- and atmospheric-scale oscillation regions, as can be seen in Sect. 7. We hope that such understanding will eventually help analyze data for leptonic unitarity tests.

In Sect. 3, we introduce the concept of parameter correlations by describing a pedagogical example of the three-neutrino system with the non-standard interactions. In Sect. 4, we give a step-by-step formulation of the perturbative framework which is to be utilized in analyzing features of the three-neutrino evolution with a non-unitary mixing matrix. The prescription for computing S matrix elements is given with the help of the tilde basis $\widetilde{S}$ matrix elements summarized in Appendix B. In Sect. 5, a general formula for the oscillation probability is derived, and applied to the computation of the appearance probability in the $\nu_\mu \to \nu_e$ channel. This section together with Appendix D.1 contains the explicit expression of the oscillation probability in the $\nu_\mu \to \nu_e$ channel to the first order in expansion parameters. In Sect. 6, we discuss the characteristic features of the correlation between the νSM CP phase and UV α parameters in the region of validity of our perturbative framework. In Sect. 7, the physics of neutrino flavor transformation with UV is discussed paying a particular attention to parameter correlation, contrasting between the regions of the solar- and atmospheric-scale enhanced oscillations. In Sect. 8, we give the concluding remarks.

3. Parameter correlation in neutrino oscillation with beyond-νSM extended settings

It may be useful to start the description of this paper by briefly recollecting some known features of parameter correlation in neutrino oscillation, in particular, in an extended setting that includes physics beyond the νSM. In this context, a general framework that is most frequently discussed is the one which includes the neutrinos' non-standard interactions (NSI) [8]

$$H_{\rm NSI} = \frac{a}{2E}\begin{bmatrix} \varepsilon_{ee} & \varepsilon_{e\mu} & \varepsilon_{e\tau} \\ \varepsilon^*_{e\mu} & \varepsilon_{\mu\mu} & \varepsilon_{\mu\tau} \\ \varepsilon^*_{e\tau} & \varepsilon^*_{\mu\tau} & \varepsilon_{\tau\tau} \end{bmatrix}, \tag{2}$$

in the flavor-basis Hamiltonian, where the ε parameters describe the flavor-dependent strengths of NSI and a denotes the matter potential (see Eq. (8)). We discuss only the so-called "propagation

NSI". For a review of the physics of NSI in wider contexts, see e.g. Refs. [50–52]. We note that the inclusion of the NSI Hamiltonian (2) brings an extra nine parameters into the νSM Hamiltonian with six degrees of freedom, the two Δm^2, the three mixing angles, and the unique CP phase, under the influence of the matter potential background.

3.1. Emergence of collective variables involving νSM and NSI parameters

A large number of parameters with UV, which is more than doubled the νSM ones, makes it conceivable that the dynamics of neutrino oscillation naturally involves rich correlations among these variables.[7] Here, we discuss only a particular type of correlation uncovered in Ref. [55] because, we believe, it illuminates the point. In that work, the authors formulated a perturbative framework of the system with NSI by using the three (the latter two assumed to be) small expansion parameters, $\epsilon \equiv \Delta m^2_{21}/\Delta m^2_{31}$, $s_{13} \equiv \sin\theta_{13}$, and the ε parameters. They derived the formulas of the oscillation probability to the second order (the third order in the $\nu_\mu \to \nu_e$ channel) in the expansion parameters, which is nothing but an extension of the Cervera et. al. formulas [56] to include NSI.[8] In this calculation the PDG convention of U_{MNS} [39] is used.

An interesting and unexpected feature of the NSI-extended formulas is the emergence of the two sets of "collective variables":

$$\begin{aligned}\Theta_{13} &\equiv s_{13}\frac{\Delta m^2_{31}}{a} + e^{i\delta}\left(s_{23}\varepsilon_{e\mu} + c_{23}\varepsilon_{e\tau}\right),\\ \Theta_{12} &\equiv \left(c_{12}s_{12}\frac{\Delta m^2_{21}}{a} + c_{23}\varepsilon_{e\mu} - s_{23}\varepsilon_{e\tau}\right)e^{i\delta},\end{aligned} \tag{3}$$

where an overall $e^{-i\delta}$ is factored out from the matrix element $S_{e\mu}$ to make the s_{13} term δ free, through which $e^{i\delta}$ dependences in Θ_{12} in Eq. (3) result. That is, if we replace $s_{13}(\Delta m^2_{31}/a)$ and $c_{12}s_{12}(\Delta m^2_{21}/a)$ in the original formulas by Θ_{13} and Θ_{12}, respectively, the extended second-order formulas with full inclusion of NSI effects automatically appear [55]. In fact, the procedure works for the third-order formula for $P(\nu_\mu \to \nu_e)$ as well. We note that the second-order computation of Ref. [55] includes the ν_μ–ν_τ sector, and the additional collective variables are identified. However, for simplicity, we do not discuss them here and refer the interested readers to Ref. [55].

The appearance of the cluster variables composed of the νSM and NSI parameters in Eq. (3) implies that there exists strong correlations between the νSM variables s_{13}–δ and the NSI $\varepsilon_{e\mu}$–$\varepsilon_{e\tau}$ parameters in such a way that they form the collective variable Θ_{13} to convert the Cervera et. al. formula to the NSI-extended version. A similar statement can be made for the other cluster variable Θ_{12} as well. The NSI-extended second-order formula derived in this way serves for understanding the s_{13}–$\varepsilon_{e\mu}$ confusion uncovered in Ref. [60] in a more complete manner, in such a way that the effects of $\varepsilon_{e\tau}$ and the CP phase δ are also included. It also predicts the occurrence of the similar correlation among the variables to produce the collective variable Θ_{12}, the feature of which could be confirmed by experiments at low energies, $(\Delta m^2_{21}/a) \sim \mathcal{O}(1)$; this possibility was revisited recently [41,42].

[7] They include the correlations between the NSI variables themselves. The examples include the ε_{ee}–$\varepsilon_{e\tau}$–$\varepsilon_{\tau\tau}$ correlation discussed in Refs. [53,54].

[8] The Cervera et. al. formula is the most commonly used probability formula in the standard three flavor mixing in matter for many purposes, e.g., in the discussion of parameter degeneracy [57–59].

Therefore, there is nothing strange in the parameter correlations among the νSM and new physics parameters. It appears that the phenomenon arises generically, at least under the environment that the matter effect is comparable to the vacuum effect.

3.2. *Dynamical nature of the parameter correlation*

We must point out, however, that the features of the parameter correlation depend on the values of the parameters involved, and also on the kinematical region of neutrino energy and baseline with background matter density. Therefore, depending upon the region of validity of the perturbative framework which is used to derive the correlation, the form of parameter correlation changes. We call all these features collectively the "*dynamical nature*" of the parameter correlation.[9]

We want to see explicitly whether a change in features of the correlation occurs when the values of the parameters involved are varied, or its effect is incorporated into the framework of perturbation theory. For this purpose let us go back to the collective variable correlation in Eg. (3). We know now the value of θ_{13} is larger than that assumed at the time the Cervera et. al. formula was derived [39]. The latest value from Daya Bay is $s_{13} = 0.148$ [61], which is of the order of $\sqrt{\epsilon} = 0.176$. Then, we need higher-order corrections of s_{13}, up to the fourth-order terms, to match to the second-order accuracy in ϵ [62,63]. When this is carried out with the inclusion of NSI [63], it is seen that part of the additional terms generated do not fit to the form of collective variables given in Eq. (3). Therefore, when we make θ_{13} larger, the parameter correlation which produced the collective variables (3) starts to dissolve.

Thus, the analysis of this particular example reveals the dynamical nature of the parameter correlation in the neutrino propagation with NSI. We expect that overseeing the results of computations of the oscillation probabilities in this and the previous papers [38] will reveal the similar dynamical behavior of the parameter correlation in the three-flavor neutrino evolution in matter with non-unitary mixing.

3.3. *Phase correlation through NSI–UV parameter correspondence?*

Can we extract information about the δ–α parameter phase correlation from the collective variables (3)? The answer is *Yes* if we assume a "uniform chemical composition model" of the matter. As far as the propagation NSI is concerned, there is one-to-one mapping between NSI ε parameters and the UV α parameters, as noticed by Blennow et. al. [26] under the assumption $N_n = N_e$—equal neutron and proton number densities in a charge-neutral medium. Of course, an extension to the more generic case of $N_e = rN_n$ [38] can be easily done without altering the conclusion. For the purpose of the present discussion, one also has to "approve" the procedure by which the $e^{i\delta}$ dependence of the collective variables (3) is fixed. That is, removing an overall phase from the matrix element $S_{e\mu}$ to make the s_{13} term δ-free, as done in Ref. [55].

Assuming that the two conditions above are met, this leads to the collective variables in Eq. (3) written by the UV α parameters,

$$\Theta_{13} = s_{13}\frac{\Delta m^2_{31}}{a} + \frac{1}{2}\left\{s_{23}\left(\bar{\alpha}_{\mu e}e^{-i\delta}\right)^* + c_{23}\left(\bar{\alpha}_{\tau e}e^{-i\delta}\right)^*\right\},$$

[9] One must be aware that our terminology of "dynamical" correlation may be different from those used in condensed matter physics or many body theory. In our case the correlated parameters are not the dynamical variables in quantum theory and there are no direct interactions between them.

$$\Theta_{12} = c_{12}s_{12}e^{i\delta}\frac{\Delta m^2_{21}}{a} + \frac{1}{2}\left\{c_{23}\left(\bar{\alpha}_{\mu e}e^{-i\delta}\right)^* - s_{23}\left(\bar{\alpha}_{\tau e}e^{-i\delta}\right)^*\right\}, \tag{4}$$

where we have to use the α parameters defined in the PDG convention of $U_{\rm MNS}$. The emerged correlation between δ and the α parameters is consistent with the canonical phase combination obtained in Ref. [38] in the PDG convention. For the relationships between the α parameters with the various $U_{\rm MNS}$ conventions, see Sect. 4.1. This is not unreasonable because the regions of validity of the perturbative frameworks in Refs. [55] and [38] overlap.

4. Formulating perturbation theory around the solar-scale enhancement with non-unitarity

The discussion of physics in this paper necessitates a new analytical framework to illuminate the effect of a non-unitary mixing matrix in the region of the solar-scale enhanced oscillations; the UV extended version of the "solar-resonance perturbation theory" [41].

4.1. Neutrino evolution in the vacuum mass eigenstate basis

As is customary in our formulation of the three active neutrino evolution in matter with UV [38], we start from the evolution equation in the vacuum mass eigenstate basis, the justification of which is given in Refs. [25,26].[10] With use of the "check basis" for the vacuum mass eigenstate basis, it takes the form of a Schrödinger equation:

$$i\frac{d}{dx}\check{\nu} = \check{H}\check{\nu} \tag{5}$$

with Hamiltonian

$$\check{H} \equiv \frac{1}{2E}\left\{\begin{bmatrix} 0 & 0 & 0 \\ 0 & \Delta m^2_{21} & 0 \\ 0 & 0 & \Delta m^2_{31}\end{bmatrix} + N^\dagger \begin{bmatrix} a-b & 0 & 0 \\ 0 & -b & 0 \\ 0 & 0 & -b\end{bmatrix} N\right\}, \tag{6}$$

where E is neutrino energy and $\Delta m^2_{ji} \equiv m^2_j - m^2_i$. A usual phase redefinition of neutrino wave function is done to leave only the mass squared differences. N denotes the non-unitary flavor mixing matrix which relates the flavor neutrino states to the vacuum mass eigenstates as

$$\nu_\beta = N_{\beta i}\check{\nu}_i, \tag{7}$$

where β (and the other Greek indices) runs over e, μ, τ, while the mass eigenstate index i (and the other Latin indices) runs over 1, 2, and 3. It must be noticed that the neutrino evolution described by Eq. (5) is unitary, as is obvious from the hermitian Hamiltonian (6). The apparent inconsistency between the unitary evolution and the non-unitarity of the flavor-basis S matrix, one of the points of emphasis in Ref. [38], will be resolved in Sect. 4.7. Note that, due to a limited number of appropriate symbols, the notations for the various bases may not always be the same in our series of papers.

The functions $a(x)$ and $b(x)$ in (17) denote the Wolfenstein matter potential [8] due to the charged current (CC) and the neutral current (NC) reactions, respectively.

$$a = 2\sqrt{2}G_F N_e E \approx 1.52 \times 10^{-4}\left(\frac{Y_e\rho}{\mathrm{g\,cm^{-3}}}\right)\left(\frac{E}{\mathrm{GeV}}\right)\mathrm{eV}^2,$$

[10] In a nutshell, Eqs. (5) with (6) describe evolution of the active three neutrinos in the 3×3 sub-space in the $(3 + N_s)$ model (as a model for low-scale UV) [24,25], or just the three-neutrino system in high-scale UV; see e.g. [26].

$$b = \sqrt{2} G_F N_n E = \frac{1}{2} \left(\frac{N_n}{N_e} \right) a. \tag{8}$$

Here, G_F is the Fermi constant, and N_e and N_n are the electron and neutron number densities in matter. ρ and Y_e denote, respectively, the matter density and the number of electrons per nucleon in matter. We define the following notations for simplicity to be used in the discussions hereafter in this paper:

$$\Delta_{ji} \equiv \frac{\Delta m^2_{ji}}{2E}, \qquad \Delta_a \equiv \frac{a}{2E}, \qquad \Delta_b \equiv \frac{b}{2E}. \tag{9}$$

For simplicity and clarity we will work with the uniform matter density approximation in this paper. However, it is not difficult to extend our treatment to a varying matter density case if adiabaticity holds.

Throughout this paper, due to the reasoning mentioned in Sect. 1, we use the SOL convention of the $U_{\rm MNS}$ matrix, the standard 3×3 unitary flavor mixing matrix

$$U_{\rm SOL} = \begin{bmatrix} 1 & 0 & 0 \\ 0 & c_{23} & s_{23} \\ 0 & -s_{23} & c_{23} \end{bmatrix} \begin{bmatrix} c_{13} & 0 & s_{13} \\ 0 & 1 & 0 \\ -s_{13} & 0 & c_{13} \end{bmatrix} \begin{bmatrix} c_{12} & s_{12} e^{i\delta} & 0 \\ -s_{12} e^{-i\delta} & c_{12} & 0 \\ 0 & 0 & 1 \end{bmatrix} \equiv U_{23} U_{13} U_{12}, \tag{10}$$

where we have used the obvious notations $s_{ij} \equiv \sin\theta_{ij}$ etc. and δ denotes the lepton KM phase [6], or the νSM CP violating phase. We use the term "SOL" because the phase factor $e^{\pm i\delta}$ is attached to the "solar angle" s_{12}. It is physically equivalent to the commonly used PDG convention [39] in which the phase factor is attached to s_{13}.

We use the α parametrization of a non-unitary mixing matrix [23] defined in the $U_{\rm SOL}$ convention:

$$N = (\mathbf{1} - \widetilde{\alpha})\, U_{\rm SOL} = \left\{ \mathbf{1} - \begin{bmatrix} \widetilde{\alpha}_{ee} & 0 & 0 \\ \widetilde{\alpha}_{\mu e} & \widetilde{\alpha}_{\mu\mu} & 0 \\ \widetilde{\alpha}_{\tau e} & \widetilde{\alpha}_{\tau\mu} & \widetilde{\alpha}_{\tau\tau} \end{bmatrix} \right\} U_{\rm SOL}. \tag{11}$$

As seen in Eq. (11), and discussed in detail in Ref. [38], the definition of the α matrix depends on the phase convention of the flavor-mixing matrix $U_{\rm MNS}$. Consistent with the notation used in Ref. [38], we denote the α matrix elements in the SOL convention as $\widetilde{\alpha}_{\beta\gamma}$.

The other convention of the MNS matrix which is heavily used in Ref. [38] is the "ATM" convention in which $e^{\pm i\delta}$ is attached to the "atmospheric angle" s_{23}:

$$U_{\rm ATM} = \begin{bmatrix} 1 & 0 & 0 \\ 0 & c_{23} & s_{23} e^{i\delta} \\ 0 & -s_{23} e^{-i\delta} & c_{23} \end{bmatrix} \begin{bmatrix} c_{13} & 0 & s_{13} \\ 0 & 1 & 0 \\ -s_{13} & 0 & c_{13} \end{bmatrix} \begin{bmatrix} c_{12} & s_{12} & 0 \\ -s_{12} & c_{12} & 0 \\ 0 & 0 & 1 \end{bmatrix}. \tag{12}$$

The α parameters defined in the ATM and PDG conventions of $U_{\rm MNS}$ are denoted as $\alpha_{\beta\gamma}$ and $\bar{\alpha}_{\beta\gamma}$, respectively, in Ref. [38], and we follow that notation in this paper. We recapitulate here the relationships between the α parameters defined with the PDG ($\bar{\alpha}$), ATM (α) and the SOL ($\widetilde{\alpha}$) conventions of $U_{\rm MNS}$:

$$\widetilde{\alpha}_{\mu e} = \bar{\alpha}_{\mu e} e^{-i\delta} = \alpha_{\mu e} e^{-i\delta},$$
$$\widetilde{\alpha}_{\tau e} = \bar{\alpha}_{\tau e} e^{-i\delta} = \alpha_{\tau e},$$

$$\widetilde{\alpha}_{\tau\mu} = \bar{\alpha}_{\tau\mu} = \alpha_{\tau\mu} e^{i\delta}. \tag{13}$$

where we note that the diagonal α parameters are equal among the three conventions.

4.2. Region of validity, expansion parameters, and the target sensitivity

In this section, we aim at constructing the perturbative framework which is valid at around the solar oscillation maximum, $\Delta m^2_{21} L/4E \sim \mathcal{O}(1)$. Given the formula

$$\frac{\Delta m^2_{21} L}{4E} = 0.953 \left(\frac{\Delta m^2_{21}}{7.5 \times 10^{-5}\text{eV}^2}\right)\left(\frac{L}{1000\,\text{km}}\right)\left(\frac{E}{100\,\text{MeV}}\right)^{-1}, \tag{14}$$

it implies neutrino energy $E = (1-5) \times 100$ MeV and baseline $L = (1-10) \times 1000$ km. In this region, the matter potential is comparable in size to the vacuum effect represented by Δm^2_{21},

$$\frac{a}{\Delta m^2_{21}} = 0.609 \left(\frac{\Delta m^2_{21}}{7.5 \times 10^{-5}\ \text{eV}^2}\right)^{-1}\left(\frac{\rho}{3.0\,\text{g/cm}^3}\right)\left(\frac{E}{200\ \text{MeV}}\right) \sim \mathcal{O}(1). \tag{15}$$

Hence, our perturbative framework must fully take into account the MSW effect caused by the Earth matter effect. A more detailed discussion of the region of validity without the UV effect is given in Ref. [41].

As in the solar resonance perturbation theory, we will have the "effective" expansion parameter in the νSM sector, $A_{\text{exp}} = c_{13}s_{13}\left(a/\Delta m^2_{31}\right) \sim 10^{-3}$, as discussed in Sect. 4.8. The reason for having such a very small expansion parameter is due to the special structure of our perturbative Hamiltonian.

To formulate our perturbative framework with UV, we use $\widetilde{\alpha}_{\beta\gamma}$, defined in Eq. (11), for the extra expansion parameters. That is, we assume that deviation from unitarity is small. Therefore, $\widetilde{\alpha}_{\beta\gamma} \ll 1$ holds for all β and γ. Though we follow basically the same procedure as in Ref. [41], we give a step-by-step presentation of the formulation because of the additional complexities associated with the inclusion of UV, and to make this paper self-contained.

What would be a reachable or a possible target sensitivity to $\widetilde{\alpha}_{\beta\gamma}$ in the context of unitarity test? For the sake of rough estimation, we assume momentarily a perfect knowledge of the νSM mixing parameters. Then, let us ask: Which level of sensitivity to UV $\widetilde{\alpha}_{\beta\gamma}$ parameters could one expect given that the accuracy of measurement of $\Delta P_{\beta\alpha} \equiv P(\nu_\beta \to \nu_\alpha) - P(\nu_\beta \to \nu_\alpha)_{\nu\text{SM}}$ (see Eq. (67)) is of the order of, for example, 10^{-2} or 10^{-4}? Notice that $\Delta P_{\beta\alpha}$ is the non-unitary contribution to the oscillation probability. The former number is more or less the situation at the current time or in the near future, while the latter is taken arbitrarily as an expectation in a foreseeable future. Since $\Delta P_{\beta\alpha} \sim \widetilde{\alpha}_{\beta\gamma}$, we would expect the constraints on $\widetilde{\alpha}_{\beta\gamma}$ parameters to be of the order of 10^{-2}, or 10^{-4}, respectively.

We note that once the accuracy of measurement reaches a "perturbative regime" the first-order UV correction is sufficient, as far as qualitative discussions are concerned. The second-order computation yields terms of the order of $\widetilde{\alpha}^2_{\beta\gamma} \sim 10^{-4}$, or $\sim 10^{-8}$, respectively, far beyond the accuracy of the $\Delta P_{\beta\alpha}$ measurement in each era. This is the reason why we restrict ourselves to the first-order formulas in this and companion papers [38].

In low-scale UV scenarios, the probability leaking term as well as the flux "mis-normalization" term in the appearance channels are of the order of $\sim |W|^4$, where W denotes collectively the active-sterile mixing matrix elements [25]. Due to unitarity in the whole $3 + N_{\text{sterile}}$ space, $\widetilde{\alpha}_{\beta\gamma}$ must be of the order of $\simeq W^2$. Then, the leaking and the mis-normalization terms are of the order of $\widetilde{\alpha}^2_{\beta\gamma} \sim 10^{-4}$

or 10^{-8} in the above two regimes, respectively, which are far too small compared to the accuracy of $\Delta P_{\beta\alpha}$ measurement in each era. This constitutes one of the serious problems in their determination.

4.3. Transformation to the tilde basis

We transform to a different basis to formulate our perturbation theory for solar-scale enhancement. It is the tilde basis

$$\widetilde{\nu}_i = (U_{12})_{ij}\,\check{\nu}_j \tag{16}$$

with Hamiltonian

$$\widetilde{H} = U_{12}\check{H}U_{12}^\dagger, \qquad \text{or} \qquad \check{H} = U_{12}^\dagger \widetilde{H} U_{12}. \tag{17}$$

Notice that the term "tilde basis" has no connection to our notation of $\widetilde{\alpha}$ parameters in the SOL convention. The Hamiltonian in the tilde basis is given by

$$\widetilde{H} = \widetilde{H}_{\nu\text{SM}} + \widetilde{H}^{(1)}_{\text{UV}} + \widetilde{H}^{(2)}_{\text{UV}}, \tag{18}$$

where each term of the right-hand side of (18) is given by

$$\widetilde{H}_{\nu\text{SM}} = \begin{bmatrix} s_{12}^2\Delta_{21} & c_{12}s_{12}e^{i\delta}\Delta_{21} & 0 \\ c_{12}s_{12}e^{-i\delta}\Delta_{21} & c_{12}^2\Delta_{21} & 0 \\ 0 & 0 & \Delta_{31} \end{bmatrix} + \begin{bmatrix} c_{13}^2\Delta_a & 0 & c_{13}s_{13}\Delta_a \\ 0 & 0 & 0 \\ c_{13}s_{13}\Delta_a & 0 & s_{13}^2\Delta_a \end{bmatrix}, \tag{19}$$

$$\widetilde{H}^{(1)}_{\text{UV}} = \Delta_b U_{13}^\dagger U_{23}^\dagger \begin{bmatrix} 2\widetilde{\alpha}_{ee}\left(1-\frac{\Delta_a}{\Delta_b}\right) & \widetilde{\alpha}^*_{\mu e} & \widetilde{\alpha}^*_{\tau e} \\ \widetilde{\alpha}_{\mu e} & 2\widetilde{\alpha}_{\mu\mu} & \widetilde{\alpha}^*_{\tau\mu} \\ \widetilde{\alpha}_{\tau e} & \widetilde{\alpha}_{\tau\mu} & 2\widetilde{\alpha}_{\tau\tau} \end{bmatrix} U_{23}U_{13}, \tag{20}$$

$$\widetilde{H}^{(2)}_{\text{UV}} = -\Delta_b U_{13}^\dagger U_{23}^\dagger \begin{bmatrix} \widetilde{\alpha}_{ee}^2\left(1-\frac{\Delta_a}{\Delta_b}\right) + |\widetilde{\alpha}_{\mu e}|^2 + |\widetilde{\alpha}_{\tau e}|^2 & \widetilde{\alpha}^*_{\mu e}\widetilde{\alpha}_{\mu\mu} + \widetilde{\alpha}^*_{\tau e}\widetilde{\alpha}_{\tau\mu} & \widetilde{\alpha}^*_{\tau e}\widetilde{\alpha}_{\tau\tau} \\ \widetilde{\alpha}_{\mu e}\widetilde{\alpha}_{\mu\mu} + \widetilde{\alpha}_{\tau e}\widetilde{\alpha}^*_{\tau\mu} & \widetilde{\alpha}_{\mu\mu}^2 + |\widetilde{\alpha}_{\tau\mu}|^2 & \widetilde{\alpha}^*_{\tau\mu}\widetilde{\alpha}_{\tau\tau} \\ \widetilde{\alpha}_{\tau e}\widetilde{\alpha}_{\tau\tau} & \widetilde{\alpha}_{\tau\mu}\widetilde{\alpha}_{\tau\tau} & \widetilde{\alpha}_{\tau\tau}^2 \end{bmatrix} U_{23}U_{13}. \tag{21}$$

In this paper, we restrict ourselves to the perturbative correction to the first order in the expansion parameters. There is a number of reasons for this limitation. It certainly simplifies our discussion of the δ–α parameter phase correlation, though we will make a brief comment on the effect of $\widetilde{H}^{(2)}_{\text{UV}}$ on the correlation in Sect. 6.2. Unfortunately, the expression of the first-order UV correction to the oscillation probability is sufficiently complex at this order, as we will see in Sects. 5.1 and 5.2 and Appendix D.1. We do not consider our restriction to the first order in $\widetilde{\alpha}_{\beta\gamma}$ a serious limitation because the framework anticipates a precision era of neutrino experiment for the unitarity test in which the condition $\widetilde{\alpha}_{\beta\gamma} \ll 1$ should be justified.

4.4. Definitions of F and K matrices

To make expressions of the S matrix and the oscillation probability as compact as possible, it is important to introduce the new matrix notations F and K:

$$F \equiv \begin{bmatrix} F_{11} & F_{12} & F_{13} \\ F_{21} & F_{22} & F_{23} \\ F_{31} & F_{32} & F_{33} \end{bmatrix} = U_{23}^{\dagger} \begin{bmatrix} 2\widetilde{\alpha}_{ee}\left(1-\frac{\Delta_a}{\Delta_b}\right) & \widetilde{\alpha}_{\mu e}^{*} & \widetilde{\alpha}_{\tau e}^{*} \\ \widetilde{\alpha}_{\mu e} & 2\widetilde{\alpha}_{\mu\mu} & \widetilde{\alpha}_{\tau\mu}^{*} \\ \widetilde{\alpha}_{\tau e} & \widetilde{\alpha}_{\tau\mu} & 2\widetilde{\alpha}_{\tau\tau} \end{bmatrix} U_{23}, \tag{22}$$

$$K = U_{13}^{\dagger} F U_{13} \equiv \begin{bmatrix} K_{11} & K_{12} & K_{13} \\ K_{21} & K_{22} & K_{23} \\ K_{31} & K_{32} & K_{33} \end{bmatrix} =$$

$$\begin{bmatrix} c_{13}^2 F_{11} + s_{13}^2 F_{33} - c_{13}s_{13}\,(F_{13}+F_{31}) & c_{13}F_{12} - s_{13}F_{32} & c_{13}^2 F_{13} - s_{13}^2 F_{31} + c_{13}s_{13}\,(F_{11}-F_{33}) \\ c_{13}F_{21} - s_{13}F_{23} & F_{22} & s_{13}F_{21} + c_{13}F_{23} \\ c_{13}^2 F_{31} - s_{13}^2 F_{13} + c_{13}s_{13}\,(F_{11}-F_{33}) & s_{13}F_{12} + c_{13}F_{32} & s_{13}^2 F_{11} + c_{13}^2 F_{33} + c_{13}s_{13}\,(F_{13}+F_{31}) \end{bmatrix}. \tag{23}$$

The explicit expressions of the elements F_{ij} and K_{ij} defined in Eqs. (22) and (23), respectively, are given in Appendix A. By using these notations, the first-order Hamiltonian in the tilde basis (20) can be written as

$$\widetilde{H}_{\rm UV}^{(1)} = \Delta_b K. \tag{24}$$

4.5. Formulating perturbation theory with the hat basis

We use the "renormalized basis" such that the zeroth-order and the perturbed Hamiltonian takes the form $\widetilde{H} = \widetilde{H}_0 + \widetilde{H}_1$. $\widetilde{H}_0$ (we discuss $\widetilde{H}_1$ later) is given by

$$\widetilde{H}_0 = \begin{bmatrix} s_{12}^2\Delta_{21} + c_{13}^2\Delta_a & c_{12}s_{12}e^{i\delta}\Delta_{21} & 0 \\ c_{12}s_{12}e^{-i\delta}\Delta_{21} & c_{12}^2\Delta_{21} & 0 \\ 0 & 0 & \Delta_{31} + s_{13}^2\Delta_a \end{bmatrix}. \tag{25}$$

To formulate the solar-resonance perturbation theory with UV, we transform to the "hat basis", which diagonalizes $\widetilde{H}_0$:

$$\hat{\nu}_i = (U_{\varphi}^{\dagger})_{ij}\widetilde{\nu}_j, \tag{26}$$

with Hamiltonian

$$\hat{H} = U_{\varphi}^{\dagger}\widetilde{H}U_{\varphi}, \tag{27}$$

where U_{φ} is parametrized as

$$U_{\varphi} = \begin{bmatrix} \cos\varphi & \sin\varphi e^{i\delta} & 0 \\ -\sin\varphi e^{-i\delta} & \cos\varphi & 0 \\ 0 & 0 & 1 \end{bmatrix}. \tag{28}$$

U_{φ} is determined such that $\hat{H}_0$ is diagonal, which leads to

$$\cos 2\varphi = \frac{\cos 2\theta_{12} - c_{13}^2 r_a}{\sqrt{\left(\cos 2\theta_{12} - c_{13}^2 r_a\right)^2 + \sin^2 2\theta_{12}}},$$

$$\sin 2\varphi = \frac{\sin 2\theta_{12}}{\sqrt{\left(\cos 2\theta_{12} - c_{13}^2 r_a\right)^2 + \sin^2 2\theta_{12}}}, \tag{29}$$

where

$$r_a \equiv \frac{a}{\Delta m_{21}^2} = \frac{\Delta_a}{\Delta_{21}}. \tag{30}$$

The three eigenvalues of the zeroth-order Hamiltonian $\widetilde{H}_0$ in (25) is given by[11]

$$\begin{aligned} h_1 &= \sin^2(\varphi - \theta_{12})\,\Delta_{21} + \cos^2\varphi c_{13}^2 \Delta_a, \\ h_2 &= \cos^2(\varphi - \theta_{12})\,\Delta_{21} + \sin^2\varphi c_{13}^2 \Delta_a, \\ h_3 &= \Delta_{31} + s_{13}^2 \Delta_a. \end{aligned} \tag{31}$$

Then, the Hamiltonian in the hat basis is given by $\hat{H} = \hat{H}_0 + \hat{H}_{\nu\mathrm{SM1}} + \hat{H}_{\mathrm{UV1}}$, where

$$\hat{H}_0 = \begin{bmatrix} h_1 & 0 & 0 \\ 0 & h_2 & 0 \\ 0 & 0 & h_3 \end{bmatrix}, \qquad \hat{H}_1^{\nu\mathrm{SM}} = \begin{bmatrix} 0 & 0 & c_\varphi c_{13} s_{13} \Delta_a \\ 0 & 0 & s_\varphi c_{13} s_{13} e^{-i\delta} \Delta_a \\ c_\varphi c_{13} s_{13} \Delta_a & s_\varphi c_{13} s_{13} e^{i\delta} \Delta_a & 0 \end{bmatrix},$$
$$\hat{H}_1^{\mathrm{UV}} = \Delta_b U_\varphi^\dagger K U_\varphi, \tag{32}$$

where the K matrix is defined in Eq. (23), and the simplified notations are hereafter used: $c_\varphi = \cos\varphi$ and $s_\varphi = \sin\varphi$. Notice that we have omitted the second-order $\hat{H}_{\mathrm{UV}}$, though one can easily compute it from (21) if necessary.

4.6. *Calculation of $\hat{S}$ and $\widetilde{S}$ matrices*

To calculate $\hat{S}(x)$ we define $\Omega(x)$ as

$$\Omega(x) = e^{i\hat{H}_0 x}\hat{S}(x). \tag{33}$$

Then, $\Omega(x)$ obeys the evolution equation

$$i\frac{d}{dx}\Omega(x) = H_1\Omega(x) \tag{34}$$

where

$$H_1 \equiv e^{i\hat{H}_0 x}\hat{H}_1 e^{-i\hat{H}_0 x}. \tag{35}$$

Notice that $\hat{H}_1 = \hat{H}_1^{\nu\mathrm{SM}} + \hat{H}_1^{\mathrm{UV}}$ as in Eq. (32). Then, $\Omega(x)$ can be computed perturbatively as

$$\Omega(x) = 1 + (-i)\int_0^x dx' H_1(x') + (-i)^2 \int_0^x dx' H_1(x') \int_0^{x'} dx'' H_1(x'') + \cdots, \tag{36}$$

[11] Notice that one can show that

$$h_1 = \frac{\Delta_{21}}{2}\left[\left(1 + c_{13}^2 r_a\right) - \sqrt{\left(\cos 2\theta_{12} - c_{13}^2 r_a\right)^2 + \sin^2 2\theta_{12}}\right],$$
$$h_2 = \frac{\Delta_{21}}{2}\left[\left(1 + c_{13}^2 r_a\right) + \sqrt{\left(\cos 2\theta_{12} - c_{13}^2 r_a\right)^2 + \sin^2 2\theta_{12}}\right].$$

and the $\hat{S}$ matrix is given by

$$\hat{S}(x) = e^{-i\hat{H}_0 x}\Omega(x). \tag{37}$$

Using $\hat{H}_1 = \hat{H}_1^{\nu\mathrm{SM}} + \hat{H}_1^{\mathrm{UV}}$ in Eq. (32), the $\hat{S}$ matrix of the νSM part is given to the zeroth and first orders in the effective expansion parameter $s_{13}\frac{\Delta_a}{h_3-h_1}$ by

$$\begin{aligned}
&\hat{S}^{(0+1)}_{\nu\mathrm{SM}}(x) = e^{-i\hat{H}_0 x}\Omega_{\nu\mathrm{SM}}(x) \\
&= \begin{bmatrix}
e^{-ih_1 x} & 0 & c_\varphi c_{13} s_{13}\frac{\Delta_a}{h_3-h_1}\left\{e^{-ih_3 x} - e^{-ih_1 x}\right\} \\
0 & e^{-ih_2 x} & s_\varphi c_{13} s_{13} e^{-i\delta}\frac{\Delta_a}{h_3-h_2}\left\{e^{-ih_3 x} - e^{-ih_2 x}\right\} \\
c_\varphi c_{13} s_{13} & s_\varphi c_{13} s_{13} e^{i\delta} & e^{-ih_3 x} \\
\frac{\Delta_a}{h_3-h_1}\left\{e^{-ih_3 x} - e^{-ih_1 x}\right\} & \frac{\Delta_a}{h_3-h_2}\left\{e^{-ih_3 x} - e^{-ih_2 x}\right\} &
\end{bmatrix},
\end{aligned} \tag{38}$$

where we have used the fact that Δ_b is spatially constant as a consequence of the uniform matter density approximation.

Then, the νSM part of the tilde basis $\widetilde{S}$ matrix is given by

$$\widetilde{S}^{(0+1)}_{\nu\mathrm{SM}} = U_\varphi \hat{S}^{(0+1)}_{\nu\mathrm{SM}} U_\varphi^\dagger = \widetilde{S}^{(0)}_{\nu\mathrm{SM}} + \widetilde{S}^{(1)}_{\nu\mathrm{SM}}, \tag{39}$$

where

$$\widetilde{S}^{(0)}_{\nu\mathrm{SM}} = \begin{bmatrix}
c_\varphi^2 e^{-ih_1 x} + s_\varphi^2 e^{-ih_2 x} & c_\varphi s_\varphi e^{i\delta}\left(e^{-ih_2 x} - e^{-ih_1 x}\right) & 0 \\
c_\varphi s_\varphi e^{-i\delta}\left(e^{-ih_2 x} - e^{-ih_1 x}\right) & s_\varphi^2 e^{-ih_1 x} + c_\varphi^2 e^{-ih_2 x} & 0 \\
0 & 0 & e^{-ih_3 x}
\end{bmatrix}. \tag{40}$$

$\widetilde{S}^{(1)}_{\nu\mathrm{SM}}$ can be written in the form

$$\widetilde{S}^{(1)}_{\nu\mathrm{SM}} = \begin{bmatrix}
0 & 0 & X \\
0 & 0 & Ye^{-i\delta} \\
X & Ye^{i\delta} & 0
\end{bmatrix}, \tag{41}$$

where

$$\begin{aligned}
X &= c_{13} s_{13}\left\{\frac{\Delta_a}{h_3-h_1} c_\varphi^2\left(e^{-ih_3 x} - e^{-ih_1 x}\right) + \frac{\Delta_a}{h_3-h_2} s_\varphi^2\left(e^{-ih_3 x} - e^{-ih_2 x}\right)\right\}, \\
Y &= c_{13} s_{13} c_\varphi s_\varphi\left\{-\frac{\Delta_a}{h_3-h_1}\left(e^{-ih_3 x} - e^{-ih_1 x}\right) + \frac{\Delta_a}{h_3-h_2}\left(e^{-ih_3 x} - e^{-ih_2 x}\right)\right\}.
\end{aligned} \tag{42}$$

Notice that $\widetilde{S}_{\nu\mathrm{SM}}$ respects the generalized T invariance.

Now, we must compute the UV parameter related part of $\hat{S}$ and $\widetilde{S}$ matrices. By remembering $\hat{H}_1^{\mathrm{UV}} = \Delta_b U_\varphi^\dagger K U_\varphi$, the UV part of H_1 in Eq. (35) is given by

$$\begin{aligned}
H_1^{\mathrm{UV}} &= e^{i\hat{H}_0 x}\hat{H}_1^{\mathrm{UV}} e^{-i\hat{H}_0 x} = \Delta_b e^{i\hat{H}_0 x} U_\varphi^\dagger K U_\varphi e^{-i\hat{H}_0 x} \\
&= \Delta_b U_\varphi^\dagger\left(U_\varphi e^{i\hat{H}_0 x} U_\varphi^\dagger\right) K\left(U_\varphi e^{-i\hat{H}_0 x} U_\varphi^\dagger\right) U_\varphi.
\end{aligned} \tag{43}$$

Due to frequent usage of the factors in the parenthesis above we give the formula for them here:

$$S_\varphi^{(\pm)} \equiv \left(U_\varphi e^{\pm i\hat{H}_0 x} U_\varphi^\dagger\right)$$

$$= \begin{bmatrix} c_\varphi^2 e^{\pm ih_1 x} + s_\varphi^2 e^{\pm ih_2 x} & c_\varphi s_\varphi e^{i\delta}\left(e^{\pm ih_2 x} - e^{\pm ih_1 x}\right) & 0 \\ c_\varphi s_\varphi e^{-i\delta}\left(e^{\pm ih_2 x} - e^{\pm ih_1 x}\right) & s_\varphi^2 e^{\pm ih_1 x} + c_\varphi^2 e^{\pm ih_2 x} & 0 \\ 0 & 0 & e^{\pm ih_3 x} \end{bmatrix}. \tag{44}$$

Notice that $\widetilde{S}^{(0)}_{\nu\mathrm{SM}}$ is nothing but $S_\varphi^{(-)}$. Then, H_1^{UV} takes a simple form:

$$H_1^{\mathrm{UV}} = \Delta_b U_\varphi^\dagger S_\varphi^{(+)} K S_\varphi^{(-)} U_\varphi \equiv \Delta_b U_\varphi^\dagger \Phi U_\varphi = \Delta_b U_\varphi^\dagger \begin{bmatrix} \Phi_{11} & \Phi_{12} & \Phi_{13} \\ \Phi_{21} & \Phi_{22} & \Phi_{23} \\ \Phi_{31} & \Phi_{32} & \Phi_{33} \end{bmatrix} U_\varphi, \tag{45}$$

where we have introduced another simplifying matrix notation $\Phi \equiv S_\varphi^{(+)} K S_\varphi^{(-)}$ and its elements Φ_{ij}. The explicit expressions of Φ_{ij} are given in Appendix A.

Since U_φ rotation back to the tilde basis removes $U_\varphi^\dagger$ and U_φ in Eq. (45), it is simpler to go directly to the calculation of the tilde basis $\widetilde{S}$ matrix:

$$\begin{aligned} \widetilde{S}(x)^{(1)}_{\mathrm{EV}} &= U_\varphi \hat{S}(x)^{(1)}_{\mathrm{EV}} U_\varphi^\dagger = U_\varphi e^{-i\hat{H}_0 x} \Omega(x)^{(1)}_{\mathrm{UV}} U_\varphi^\dagger = \Delta_b U_\varphi e^{-i\hat{H}_0 x} U_\varphi^\dagger \left[(-i)\int_0^x dx' \Phi(x')\right] \\ &= \Delta_b S_\varphi^{(-)} (-i) \int_0^x dx' \begin{bmatrix} \Phi_{11}(x') & \Phi_{12}(x') & \Phi_{13}(x') \\ \Phi_{21}(x') & \Phi_{22}(x') & \Phi_{23}(x') \\ \Phi_{31}(x') & \Phi_{32}(x') & \Phi_{33}(x') \end{bmatrix}. \end{aligned} \tag{46}$$

Hereafter, the subscript "EV" is used for the $\widetilde{S}$ and $\hat{S}$ matrices to indicate that they describe unitary evolution. We note that the subscript "UV" placed on $\Omega(x)^{(1)}_{\mathrm{UV}}$ implies that it is the first-order contribution from the UV part of H_1, not to be confused with the "UV" subscript showing the genuine non-unitary nature of the part of the probability which will be defined in Eq. (56). The computed results of the elements of $\widetilde{S}(x)^{(1)}_{\mathrm{EV}}$ are given in Appendix B. Notice that again $\widetilde{S}(x)^{(1)}_{\mathrm{EV}}$ respects the generalized T invariance.

Thus, we have computed all the tilde-basis S matrix elements to the first order as

$$\widetilde{S} = \widetilde{S}^{(0)}_{\nu\mathrm{SM}} + \widetilde{S}^{(1)}_{\nu\mathrm{SM}} + \widetilde{S}^{(1)}_{\mathrm{EV}}. \tag{47}$$

The first and the second terms are given, respectively, in Eqs. (40) and (41) with (42), and the third in Appendix B.

4.7. The relations between various bases and computation of the flavor-basis S matrix

We first summarize the relationship between the flavor basis, the check (vacuum mass eigenstate) basis, the tilde, and the hat (zeroth-order diagonalized Hamiltonian) basis. Only the unitary transformations are involved in changing from the hat basis to the tilde basis, and from the tilde basis to the check basis:

$$\begin{aligned} &\hat{H} = U_\varphi^\dagger \widetilde{H} U_\varphi, \qquad \text{or} \qquad \widetilde{H} = U_\varphi \hat{H} U_\varphi^\dagger, \\ &\widetilde{H} = U_{12} \check{H} U_{12}^\dagger, \qquad \text{or} \qquad \check{H} = U_{12}^\dagger \widetilde{H} U_{12} = U_{12}^\dagger U_\varphi \hat{H} U_\varphi^\dagger U_{12}. \end{aligned} \tag{48}$$

The non-unitary transformation is involved from the check basis to the flavor basis:

$$\nu_\beta = N_{\beta i} \check{\nu}_i = \{(1 - \widetilde{\alpha}) U\}_{\beta i} \check{\nu}_i. \tag{49}$$

The relationship between the flavor basis Hamiltonian $H_{\rm flavor}$ and the hat basis one $\hat{H}$ is

$$\begin{aligned} H_{\rm flavor} &= \{(1-\widetilde{\alpha})U\}\,\check{H}\,\{(1-\widetilde{\alpha})U\}^\dagger = (1-\widetilde{\alpha})UU_{12}^\dagger U_\varphi \hat{H} U_\varphi^\dagger U_{12} U^\dagger (1-\widetilde{\alpha})^\dagger \\ &= (1-\widetilde{\alpha})U_{23}U_{13}U_\varphi \hat{H} U_\varphi^\dagger U_{13}^\dagger U_{23}^\dagger (1-\widetilde{\alpha})^\dagger. \end{aligned} \tag{50}$$

Then, the flavor-basis S matrix is related to $\hat{S}$ and $\widetilde{S}$ matrices as

$$\begin{aligned} S_{\rm flavor} &= (1-\widetilde{\alpha})U_{23}U_{13}U_\varphi \hat{S} U_\varphi^\dagger U_{13}^\dagger U_{23}^\dagger (1-\widetilde{\alpha})^\dagger \\ &= (1-\widetilde{\alpha})U_{23}U_{13}\widetilde{S} U_{13}^\dagger U_{23}^\dagger (1-\widetilde{\alpha})^\dagger. \end{aligned} \tag{51}$$

Using the formula (51), it is straightforward to compute the flavor-basis S matrix elements. Notice, however, that U_{13} is free from CP phase δ due to our choice of the SOL convention of the $U_{\rm MNS}$ matrix in Eq. (10).

The flavor-basis S matrix has the structure $S_{\rm flavor} = (1-\widetilde{\alpha})S_{\rm prop}(1-\widetilde{\alpha})^\dagger$ where $S_{\rm prop} \equiv U_{23}U_{13}\widetilde{S}U_{13}^\dagger U_{23}^\dagger$ describes the unitary evolution despite the presence of non-unitary mixing [38]. The factors $(1-\widetilde{\alpha})$ and $(1-\widetilde{\alpha})^\dagger$, parts of the N matrix which project the mass eigenstates to the flavor states and vice versa, may be interpreted as playing the analogous roles as the "production NSI" and "detection NSI" which induce non-unitarity [64]. Notice, however, that the production and detection NSI in this case are not independent from the "propagation NSI", but are solely determined by the latter.

4.8. Effective expansion parameter with and without the UV effect

As announced in Sect. 4.2, the expression of $\widetilde{S}^{(1)}_{\nu\rm SM}$ in Eq. (41) with (42) tells us that we have another expansion parameter [41]

$$A_{\rm exp} \equiv c_{13}s_{13}\left|\frac{a}{\Delta m^2_{31}}\right| = 2.78\times 10^{-3}\left(\frac{\Delta m^2_{31}}{2.4\times 10^{-3}\ {\rm eV}^2}\right)^{-1}\left(\frac{\rho}{3.0\ {\rm g/cm}^3}\right)\left(\frac{E}{200\ {\rm MeV}}\right), \tag{52}$$

which is very small. The reason for such a "generated by the framework" expansion parameter is the special feature of the perturbed Hamiltonian in Eq. (32).

In fact, our perturbative framework is peculiar from the beginning, in the sense that the key non-perturbed part of the Hamiltonian (25), its top-left 2×2 sub-matrix, is smaller in size than the 33-element by a factor of $\sim$ 30, and is comparable with $\hat{H}_1^{\nu\rm SM}$ in Eq. (32). The secret for the emergence of the very small effective expansion parameter (52) is that the 33-element decouples in the leading order and appears in the perturbative corrections only in the energy denominator, making them *smaller for the larger ratio* of $\Delta m^2_{31}/\Delta m^2_{21}$. The latter property holds because of the special structure of perturbative Hamiltonian $\hat{H}_1^{\nu\rm SM}$ with non-vanishing elements only in the third row and third column.

With the inclusion of the UV Hamiltonian (24), however, the size of the first-order correction is controlled not only by $A_{\rm exp}$ in Eq. (52) but also by the magnitudes of $\widetilde{\alpha}_{\beta,\gamma}$. In computing the higher-order corrections the energy denominator suppression does not work for all the terms because the last property, "non-vanishing elements in the third row and third column only", ceases to hold in the first-order Hamiltonian. This is confirmed by looking into the formulas of the oscillation probabilities in Sect. 5.1, Appendix D.1, and Sect. 5.2.

5. Neutrino oscillation probability to the first order in expansion

The oscillation probability can be calculated using the formula

$$P(\nu_\beta \to \nu_\alpha) = |(S_{\rm flavor})_{\alpha\beta}|^2. \tag{53}$$

We denote the flavor-basis S matrices corresponding to $\widetilde{S}^{(0)}_{\nu{\rm SM}}$, $\widetilde{S}^{(1)}_{\nu{\rm SM}}$ and $\widetilde{S}^{(1)}_{\rm EV}$ as $S^{(0)}_{\nu{\rm SM}}$, $S^{(1)}_{\nu{\rm SM}}$ and $S^{(1)}_{\rm EV}$, respectively, as they are related through Eq. (51). To the first order we have

$$S_{\rm flavor} = S^{(0)}_{\nu{\rm SM}} + S^{(1)}_{\nu{\rm SM}} + S^{(1)}_{\rm EV} - \widetilde{\alpha} S^{(0)}_{\nu{\rm SM}} - S^{(0)}_{\nu{\rm SM}} \widetilde{\alpha}^\dagger. \tag{54}$$

Then, we are ready to calculate the expressions of the oscillation probabilities using the formula (53) to the first order in the expansion parameters. Following Ref. [38], we categorize $P(\nu_\beta \to \nu_\alpha)$ into the three types of terms:

$$P(\nu_\beta \to \nu_\alpha) = P(\nu_\beta \to \nu_\alpha)^{(0+1)}_{\nu{\rm SM}} + P(\nu_\beta \to \nu_\alpha)^{(1)}_{\rm EV} + P(\nu_\beta \to \nu_\alpha)^{(1)}_{\rm UV}, \tag{55}$$

where

$$\begin{aligned}
P(\nu_\beta \to \nu_\alpha)^{(0+1)}_{\nu{\rm SM}} &= \left|\left(S^{(0)}_{\nu{\rm SM}}\right)_{\alpha\beta}\right|^2 + 2{\rm Re}\left[\left(S^{(0)}_{\nu{\rm SM}}\right)^*_{\alpha\beta}\left(S^{(1)}_{\nu{\rm SM}}\right)_{\alpha\beta}\right], \\
P(\nu_\beta \to \nu_\alpha)^{(1)}_{\rm EV} &= 2{\rm Re}\left[\left(S^{(0)}_{\nu{\rm SM}}\right)^*_{\alpha\beta}\left(S^{(1)}_{\rm EV}\right)_{\alpha\beta}\right], \\
P(\nu_\beta \to \nu_\alpha)^{(1)}_{\rm UV} &= -2{\rm Re}\left[\left(S^{(0)}_{\nu{\rm SM}}\right)^*_{\alpha\beta}\left(\widetilde{\alpha} S^{(0)}_{\nu{\rm SM}} + S^{(0)}_{\nu{\rm SM}}\widetilde{\alpha}^\dagger\right)_{\alpha\beta}\right].
\end{aligned} \tag{56}$$

The subscripts "EV" and "UV" refer the unitary evolution part and the genuine non-unitary contribution, terminology defined in Ref. [38]. The first term in Eq. (56), $P(\nu_\beta \to \nu_\alpha)^{(0+1)}_{\nu{\rm SM}}$, is already computed in Ref. [41]. Hence, we do not repeat the calculation, but urge the readers to go to this reference. Notice that use of the SOL convention of $U_{\rm MNS}$ does not alter the expression of the oscillation probabilities. The rest of the terms in Eq. (56) can be computed straightforwardly using the expressions of the tilde-basis S matrix which are given explicitly in Appendix B, and the $\widetilde{\alpha}$ matrix defined in Eq. (11).

Unfortunately, the resulting expression of the oscillation probability even at first order is far from simple. Therefore, to give a feeling to the readers, we will show in the next two subsections a part of the first-order probability in the $\nu_\mu \to \nu_e$ channel. In Sect. 5.1, one of the five terms in $P(\nu_\mu \to \nu_e)^{(1)}_{\rm EV}$ is given, and the whole expression of $P(\nu_\mu \to \nu_e)^{(1)}_{\rm UV}$ is in Sect. 5.2. We leave the rest of the terms of $P(\nu_\mu \to \nu_e)^{(1)}_{\rm EV}$ to Appendix D.1. In this appendix, we also give a practical suggestion to the readers on how to compute the oscillation probabilities in the ν_μ–ν_τ sector.

For notational simplicity, we define, following Ref. [41], the reduced Jarlskog factor in matter as

$$J_{mr} \equiv c_{23}s_{23}c^2_{13}s_{13}c_\varphi s_\varphi = J_r\left[\left(\cos 2\theta_{12} - c^2_{13}r_a\right)^2 + \sin^2 2\theta_{12}\right]^{-1/2}, \tag{57}$$

which is proportional to the reduced Jarlskog factor in vacuum, $J_r \equiv c_{23}s_{23}c^2_{13}s_{13}c_{12}s_{12}$ [65]. We have used Eq. (29) in the second equality in (57).

In this paper, we do not discuss numerical accuracy of the first-order oscillation probability because (1) the νSM part, which is controlled by $A_{\rm exp} \sim 10^{-3}$, is known to be very accurate already in the

first order [41], and (2) the accuracy of the UV-related part is trivial; the smaller the $\alpha_{\beta\gamma}$, the better the accuracy.[12]

5.1. *Unitary evolution part of the first-order probability* $P(\nu_\mu \to \nu_e)^{(1)}_{EV}$

We first introduce the decomposition of $P(\nu_\mu \to \nu_e)^{(1)}_{\rm EV}$. After computation of all the terms, we assemble them according to the types of K_{ij} variables involved. See Eq. (23) and (A2) in Appendix A for the definitions and the explicit expressions of the K_{ij}, respectively. For bookkeeping purposes we decompose $P(\nu_\mu \to \nu_e)^{(1)}_{\rm EV}$ into the following four terms:

$$P(\nu_\mu \to \nu_e)^{(1)}_{\rm EV} = P(\nu_\mu \to \nu_e)^{(1)}_{\rm EV}|_{\text{D-OD}} + P(\nu_\mu \to \nu_e)^{(1)}_{\rm EV}|_{\text{OD1}} P(\nu_\mu \to \nu_e)^{(1)}_{\rm EV}|_{\text{OD2}} + P(\nu_\mu \to \nu_e)^{(1)}_{\rm EV}|_{\text{OD3}}, \tag{58}$$

where the subscripts "D" and "OD" refer to the diagonal and the off-diagonal K_{ij} variables. The organization inside each term is largely determined such that the symmetry under the transformation $\varphi \to \varphi + (\pi/2)$ is manifest. See Sect. 5.3 for the φ symmetry.

Here, we only present the first term in Eq. (58), $P(\nu_\mu \to \nu_e)^{(1)}_{\rm EV}|_{\text{D-OD}}$, leaving the others to Appendix D.1:

$$\begin{aligned}
&P(\nu_\mu \to \nu_e)^{(1)}_{\rm EV}|_{\text{D-OD}} \\
&= 4J_{mr} \sin\delta \cos 2\varphi\, (K_{22} - K_{11})\, (\Delta_b x) \sin^2 \frac{(h_2 - h_1)x}{2} \\
&+ 2\,(K_{33} - K_{11})\,(\Delta_b x) \Bigg[J_{mr} \cos\delta \sin(h_2 - h_1)x - 2 s^2_{23} c_{13} s_{13} \left\{ c^2_\varphi \sin(h_3 - h_1)x + s^2_\varphi \sin(h_3 - h_2)x \right\} \Bigg] \\
&+ 4J_{mr}\,(K_{33} - K_{22})\,(\Delta_b x) \\
&\times \left[2\cos\delta \sin\frac{(h_3 - h_2)x}{2} \sin\frac{(h_2 - h_1)x}{2} \sin\frac{(h_1 - h_3)x}{2} + \sin\delta \left\{ \sin^2\frac{(h_3 - h_2)x}{2} - \sin^2\frac{(h_3 - h_1)x}{2} \right\} \right] \\
&+ \left[\cos 2\varphi\, (K_{22} - K_{11}) + \sin 2\varphi \left(K_{12} e^{-i\delta} + K_{21} e^{i\delta} \right) \right] (\Delta_b x) \\
&\times \Bigg[2 c_{13} c^2_\varphi s^2_\varphi \left\{ c^2_{23} c_{13} \sin(h_2 - h_1)x - 4 s^2_{23} s_{13} \sin\frac{(h_3 - h_2)x}{2} \sin\frac{(h_2 - h_1)x}{2} \sin\frac{(h_1 - h_3)x}{2} \right\} \\
&+ 2J_{mr} \cos\delta \left[c^2_\varphi \sin(h_3 - h_1)x + s^2_\varphi \sin(h_3 - h_2)x \right] \\
&- 4J_{mr} \sin\delta \left\{ c^2_\varphi \sin^2\frac{(h_3 - h_1)x}{2} + s^2_\varphi \sin^2\frac{(h_3 - h_2)x}{2} - 4 c^2_\varphi s^2_\varphi \sin^2\frac{(h_2 - h_1)x}{2} \right\} \Bigg] \\
&+ 2 \left[\sin 2\varphi\, (K_{22} - K_{11}) - \cos 2\varphi \left(K_{12} e^{-i\delta} + K_{21} e^{i\delta} \right) \right] \\
&\times \Bigg[s^2_{23} c_{13} s_{13} c_\varphi s_\varphi \Bigg\{ (\Delta_b x) \left[c^2_\varphi \sin(h_3 - h_1)x + s^2_\varphi \sin(h_3 - h_2)x \right] \\
&+ 2\frac{\Delta_b}{h_2 - h_1} \left[\sin^2\frac{(h_3 - h_2)x}{2} - \sin^2\frac{(h_3 - h_1)x}{2} - \cos 2\varphi \sin^2\frac{(h_2 - h_1)x}{2} \right] \Bigg\}
\end{aligned}$$

[12] If we set the target accuracy for the unitarity test at a % level, $\alpha_{\beta\gamma} \lesssim 10^{-2}$. Then, within the accuracy of the νSM part, $10^{-3} \lesssim \alpha_{\beta\gamma} \lesssim 10^{-2}$, the second-order UV corrections could play a role. However, it is of the order of $\sim \alpha^2_{\beta\gamma} \lesssim 10^{-4}$, and hence it is negligible.

$$
\begin{aligned}
&+ 4J_{mr}\cos\delta c_\varphi s_\varphi \frac{\Delta_b}{h_2-h_1}\sin^2\frac{(h_2-h_1)x}{2}\Bigg] \\
&- 4c_{23}c_{13}^2 c_\varphi s_\varphi \left[\cos 2\varphi\,(K_{22}-K_{11}) + \sin 2\varphi\left(K_{12}e^{-i\delta}+K_{21}e^{i\delta}\right)\right] \\
&\times \frac{\Delta_b}{h_2-h_1}\Bigg[-s_{23}\cos\delta\left\{\sin^2\frac{(h_3-h_2)x}{2}-\sin^2\frac{(h_3-h_1)x}{2}-\cos 2\varphi\sin^2\frac{(h_2-h_1)x}{2}\right\} \\
&+ c_{23}\sin 2\varphi\sin^2\frac{(h_2-h_1)x}{2}+2s_{23}\sin\delta\sin\frac{(h_3-h_2)x}{2}\sin\frac{(h_2-h_1)x}{2}\sin\frac{(h_1-h_3)x}{2}\Bigg] \\
&+ 2J_{mr}c_\varphi s_\varphi\left[\sin 2\varphi\,(K_{22}-K_{11}) - \cos 2\varphi\left(K_{12}e^{-i\delta}+K_{21}e^{i\delta}\right)\right](\Delta_b x) \\
&\times\Bigg[-\left\{\cos\delta\sin(h_2-h_1)x+2\sin\delta\cos 2\varphi\sin^2\frac{(h_2-h_1)x}{2}\right\} \\
&+ 2\sin\delta\left\{\sin^2\frac{(h_3-h_2)x}{2}-\sin^2\frac{(h_3-h_1)x}{2}-\cos 2\varphi\sin^2\frac{(h_2-h_1)x}{2}\right\} \\
&+ 4\cos\delta\sin\frac{(h_3-h_2)x}{2}\sin\frac{(h_2-h_1)x}{2}\sin\frac{(h_1-h_3)x}{2}\Bigg]. \qquad (59)
\end{aligned}
$$

We first note that the α parameter dependence is expressed through the K_{jj} elements; see its definition and the expression Eq. (23) and (A2), respectively. It is noticeable that the diagonal K_{jj} elements organize themselves into the form of difference, $K_{22}-K_{11}$ type combinations, as it should be, because it comes from the rephasing invariance.[13] This leads to the similar structure expressed by the diagonal α parameters; see Sect. 6.1.

5.2. *Non-unitary part of the first-order probability* $P(\nu_\mu \to \nu_e)^{(1)}_{UV}$

To calculate $P(\nu_\mu \to \nu_e)^{(1)}_{\rm UV}$ defined in the last line in Eq. (56), we need the expressions of zeroth-order elements of νSM matrix $S^{(0)}_{\nu\rm SM}$, which are given in Appendix C. They can be easily obtained from the tilde-basis S matrix in Eq. (40). Using the $S^{(0)}$ matrix elements $P(\nu_\mu \to \nu_e)^{(1)}_{\rm UV}$ can be readily calculated as

$$
\begin{aligned}
&P(\nu_\mu \to \nu_e)^{(1)}_{\rm UV} = -2(\widetilde{\alpha}_{ee}+\widetilde{\alpha}_{\mu\mu})|S^{(0)}_{e\mu}|^2 - 2{\rm Re}\left[\widetilde{\alpha}_{\mu e}(S^{(0)}_{ee})^* S^{(0)}_{e\mu}\right] \\
&= -2(\widetilde{\alpha}_{ee}+\widetilde{\alpha}_{\mu\mu})\Bigg[c_{23}^2c_{13}^2\sin^2 2\varphi\sin^2\frac{(h_2-h_1)x}{2} \\
&+ s_{23}^2\sin^2 2\theta_{13}\left\{c_\varphi^2\sin^2\frac{(h_3-h_1)x}{2}+s_\varphi^2\sin^2\frac{(h_3-h_2)x}{2}-c_\varphi^2 s_\varphi^2\sin^2\frac{(h_2-h_1)x}{2}\right\} \\
&+ 4J_{mr}\cos\delta\left\{\cos 2\varphi\sin^2\frac{(h_2-h_1)x}{2}-\sin^2\frac{(h_3-h_2)x}{2}+\sin^2\frac{(h_3-h_1)x}{2}\right\} \\
&+ 8J_{mr}\sin\delta\sin\frac{(h_3-h_2)x}{2}\sin\frac{(h_2-h_1)x}{2}\sin\frac{(h_1-h_3)x}{2}\Bigg] \\
&+ {\rm Re}(\widetilde{\alpha}_{\mu e})\Bigg[2c_{23}c_{13}\sin 2\varphi\cos\delta\left(c_{13}^2\cos 2\varphi\sin^2\frac{(h_2-h_1)x}{2}+s_{13}^2\left\{\sin^2\frac{(h_3-h_2)x}{2}-\sin^2\frac{(h_3-h_1)x}{2}\right\}\right) \\
&- c_{23}c_{13}\sin 2\varphi\sin\delta\left(c_{13}^2\sin(h_2-h_1)x - s_{13}^2\left\{\sin(h_3-h_2)x-\sin(h_3-h_1)x\right\}\right)
\end{aligned}
$$

[13] The fact is well known in the systems with the NSI parameters $\varepsilon_{\beta\gamma}$. For a demonstration of the $\varepsilon_{\beta\beta}-\varepsilon_{\gamma\gamma}$ structure to the third order in the NSI parameters, see Ref. [55], in particular its arXiv v1 for the explicit form.

$$
\begin{aligned}
&- s_{23}\sin 2\theta_{13}\left(c_{13}^2\sin^2 2\varphi\sin^2\frac{(h_2-h_1)x}{2} - 2\cos 2\theta_{13}\left\{c_\varphi^2\sin^2\frac{(h_3-h_1)x}{2} + s_\varphi^2\sin^2\frac{(h_3-h_2)x}{2}\right\}\right)\Bigg] \\
&- \mathrm{Im}(\widetilde{\alpha}_{\mu e})\Bigg[c_{23}c_{13}\sin 2\varphi\cos\delta\left(c_{13}^2\sin(h_2-h_1)x - s_{13}^2\left\{\sin(h_3-h_2)x - \sin(h_3-h_1)x\right\}\right) \\
&+ 2c_{23}c_{13}\sin 2\varphi\sin\delta\left(c_{13}^2\cos 2\varphi\sin^2\frac{(h_2-h_1)x}{2} + s_{13}^2\left\{\sin^2\frac{(h_3-h_2)x}{2} - \sin^2\frac{(h_3-h_1)x}{2}\right\}\right) \\
&+ s_{23}\sin 2\theta_{13}\left\{c_\varphi^2\sin(h_3-h_1)x + s_\varphi^2\sin(h_3-h_2)x\right\}\Bigg]. \qquad (60)
\end{aligned}
$$

Here, the dependence on the $\alpha_{\beta\gamma}$ is manifest. The feature of the diagonal α parameter correlation is vastly different from that of the unitary evolution part $P(\nu_\mu \to \nu_e)^{(1)}_{\mathrm{EV}}$, as will be discussed in Sect. 6.1.

5.3. *Symmetry of the oscillation probability*

It is observed in Ref. [41] that for each matter-dressed mixing angle ϕ there is an invariance under the transformation $\phi \to \phi + (\pi/2)$. ϕ can be θ_{13} or θ_{12} in matter.[14] In our system in this paper, the oscillation probability is invariant under the transformation

$$
\varphi \to \varphi + \frac{\pi}{2}, \qquad (61)
$$

which induces the following transformations simultaneously:

$$
\begin{aligned}
&h_1 \to h_2, \qquad h_2 \to h_1, \\
&c_\varphi \to -s_\varphi, \qquad s_\varphi \to +c_\varphi, \qquad \cos 2\varphi \to -\cos 2\varphi, \qquad \sin 2\varphi \to -\sin 2\varphi. \qquad (62)
\end{aligned}
$$

Hence, $J_{mr} \to -J_{mr}$ under the transformation.

It is interesting to observe explicitly that the symmetry is respected by $P(\nu_\mu \to \nu_e)^{(1)}_{\mathrm{EV}}$ and $P(\nu_\mu \to \nu_e)^{(1)}_{\mathrm{UV}}$, the former of which is given in Sect. 5.1 and Appendix D.1, and the latter in Sect. 5.2. The nature of the symmetry is identified as the "dynamical symmetry", not a symmetry in the Hamiltonian [41]. Yet, it serves for a powerful consistency check of the calculation.

6. Dynamical correlation between νSM and the UV α parameters

In this section, we discuss correlations between νSM and the UV α parameters, including the clustering of the latter, which are manifested in the oscillation probabilities calculated in Sects. 5.1, 5.2 and Appendix D.1.[15]

6.1. *Diagonal α parameter correlation*

As discussed in Ref. [38], the diagonal α parameters have particular types of correlations in the evolution part of the probability

$$
\left(\frac{\Delta_a}{\Delta_b} - 1\right)\alpha_{ee} + \alpha_{\mu\mu}, \qquad \text{and} \qquad \alpha_{\mu\mu} - \alpha_{\tau\tau}, \qquad (63)
$$

[14] The θ_{12} counterpart has previously been noticed in Ref. [66].

[15] For most of our purposes, the expressions of the flavor-basis S matrix, S_{flavor}, are sufficiently informative, but not for the diagonal α parameter correlation, the discussion of which requires rephasing invariant quantities.

which arises due to the rephasing invariance. It becomes manifest in the would-be flavor basis $H_{\text{wb-flavor}} \equiv U\check{H}U^\dagger = U_{23}\widetilde{H}U_{23}^\dagger$. Of course, it must hold in regions of the solar-scale enhanced oscillation. In our expressions of $P(\nu_\mu \to \nu_e)^{(1)}_{\text{EV}}$ given in Sect. 5.1 and in Appendix D.1, it is hidden in the diagonal K_{jj} parameters in the form of $K_{jj} - K_{ii}$:[16]

$$\begin{aligned}
K_{22} - K_{11} &= 2c_{13}^2\left[\widetilde{\alpha}_{ee}\left(\frac{\Delta_a}{\Delta_b} - 1\right) + \widetilde{\alpha}_{\mu\mu}\right] - 2(s_{23}^2 - c_{23}^2 s_{13}^2)(\widetilde{\alpha}_{\mu\mu} - \widetilde{\alpha}_{\tau\tau}) \\
&\quad - 2(1 + s_{13}^2)c_{23}s_{23}\text{Re}\left(\widetilde{\alpha}_{\tau\mu}\right) + 2c_{13}s_{13}\text{Re}\left(s_{23}\widetilde{\alpha}_{\mu e} + c_{23}\widetilde{\alpha}_{\tau e}\right) \\
K_{33} - K_{22} &= -2s_{13}^2\left[\widetilde{\alpha}_{ee}\left(\frac{\Delta_a}{\Delta_b} - 1\right) + \widetilde{\alpha}_{\mu\mu}\right] + 2(s_{23}^2 - c_{23}^2 c_{13}^2)(\widetilde{\alpha}_{\mu\mu} - \widetilde{\alpha}_{\tau\tau}) \\
&\quad + 2(1 + c_{13}^2)c_{23}s_{23}\text{Re}\left(\widetilde{\alpha}_{\tau\mu}\right) + 2c_{13}s_{13}\text{Re}\left(s_{23}\widetilde{\alpha}_{\mu e} + c_{23}\widetilde{\alpha}_{\tau e}\right). \qquad (64)
\end{aligned}$$

We note that $K_{33} - K_{11}$ is not independent of the above two expressions as it is obtained by adding them. See (23) for definition of K_{ij}, and Appendix A for their explicit expressions. Though the diagonal α parameter correlation is written in terms of the SOL convention $\widetilde{\alpha}_{jj}$ variables, it is independent of the convention of U_{MNS} because the variables do not depend on the convention.

6.2. *Correlations between νSM phase δ and the α parameters*

In view of the expressions of the first-order probability and its UV-related but unitary part in Sect. 5.1 and Appendix D.1, we identify the following correlated pairs consisting of the δ–α parameters, $K_{12}e^{-i\delta}$ and $K_{23}e^{i\delta}$, where the blobs of the α parameters K_{12} and K_{23} can be written as

$$\begin{aligned}
K_{12}e^{-i\delta} &= c_{13}\left\{c_{23}\left(\widetilde{\alpha}_{\mu e}e^{i\delta}\right)^* - s_{23}\left(\widetilde{\alpha}_{\tau e}e^{i\delta}\right)^*\right\} - s_{13}e^{-i\delta}\left[2c_{23}s_{23}(\widetilde{\alpha}_{\mu\mu} - \widetilde{\alpha}_{\tau\tau}) + c_{23}^2\widetilde{\alpha}_{\tau\mu} - s_{23}^2\widetilde{\alpha}_{\tau\mu}^*\right], \\
K_{23}e^{i\delta} &= s_{13}\left\{c_{23}\left(\widetilde{\alpha}_{\mu e}e^{i\delta}\right) - s_{23}\left(\widetilde{\alpha}_{\tau e}e^{i\delta}\right)\right\} + c_{13}e^{i\delta}\left[2c_{23}s_{23}(\widetilde{\alpha}_{\mu\mu} - \widetilde{\alpha}_{\tau\tau}) + c_{23}^2\widetilde{\alpha}_{\tau\mu}^* - s_{23}^2\widetilde{\alpha}_{\tau\mu}\right]. \qquad (65)
\end{aligned}$$

Therefore, the δ–complex-α parameter correlation *does exist* in the SOL convention of U_{MNS}, which is in marked contrast to the feature of no δ–α parameter phase correlation in the region of the atmospheric scale enhanced oscillation [38]. Notice that $K_{21}e^{i\delta} = \left(K_{12}e^{-i\delta}\right)^*$ and $K_{32}e^{-i\delta} = \left(K_{23}e^{i\delta}\right)^*$, and therefore they do not introduce correlations independent of those in Eq. (65). In fact, the feature of the $e^{\pm i\delta}$–K blob correlation can be traced back to the form of Φ_{ij} given in Appendix A.

One can also conclude from the features of $\widetilde{\alpha}_{\mu e}$ vs $e^{\pm i\delta}$ correlation seen in Eq. (64) and (65) there is no definite "chiral" combination $\widetilde{\alpha}_{\mu e}e^{i\delta}$ and/or $\widetilde{\alpha}_{\tau e}e^{i\delta}$, nor $\widetilde{\alpha}_{\tau\mu}e^{\pm i\delta}$. Consideration of the non-unitary part of the probability (60) does not change the conclusion.

To summarize, the feature of the δ–α parameter correlation at around the solar scale enhanced oscillation is different from the one in the region of the atmospheric scale oscillation discussed in Ref. [38], most notably, in the following two aspects:

- The correlation between the νSM phase δ and the α parameters does exist in the SOL convention of U_{MNS} in the region of the solar scale enhanced oscillation.
- However, the correlation does not have the "chiral" form, $\widetilde{\alpha}_{\beta\gamma}e^{\pm i\delta}$. Rather it takes the form of correlation between $e^{\pm i\delta}$ and the blobs composed of the α parameters.

[16] We refer to the UV parameters, in generic contexts, as the "α parameters", but use the notation "$\widetilde{\alpha}$" in making the statements about the formulas and the results obtained by using the SOL convention of U_{MNS}.

Since the correlation between δ and the K_{12}–K_{23} cluster variables lives in Φ matrix elements, which are the building block of the perturbation series, it is obvious that the correlation prevails to higher orders in perturbation theory in the unitary evolution part.

6.3. *Nature of the δ–α parameter correlation: Is it real?*

The result in Ref. [38] shows that the SOL convention of $U_{\rm MNS}$ is the unique case in the atmospheric-scale enhanced oscillation in which the δ–α parameter correlation is absent. Then, the first itemized statement above indicates that there is no $U_{\rm MNS}$ convention in which the phase correlation is absent both at around the atmospheric- and the solar-scale enhanced oscillations. Thus we can now conclude that the δ–α parameter correlations seen in this and the previous paper [38] are all physical. That is, it cannot be wiped away by a $U_{\rm MNS}$ convention choice.

In fact, it is very likely that, in the solar-scale enhanced oscillation region, the phase correlation exists with all three conventions of $U_{\rm MNS}$. The oscillation probability in the other $U_{\rm MNS}$ conventions can be obtained simply by using the translation rule, Eq. (13).[17] Then, we observe in the ATM and PDG conventions even more complicated correlations between $e^{\pm i\delta}$ and the blobs composed of the α parameters inside which some of the α parameters are attached with $e^{\pm i\delta}$.

One may wonder why the features of the correlation between δ and the α parameters are so different between the regions of the atmospheric- and the solar-scale enhanced oscillations, but it is entirely normal. As we have learned in Sect. 3, the nature of the parameter correlation in neutrino evolution with the inclusion of outside-νSM ingredients is dynamical. The features depend on the values of the relevant parameters as well as the kinematical regions where different degrees of freedom play the dominant role. The dynamical nature of the phase correlation will be demonstrated in a visible way in Sect. 7.

6.4. *Clustering of the α parameters*

In addition to the $\delta-$(blob of the α parameters) correlation, we observe a feature which may be called the "clustering of the α parameters" in the unitary evolution part of the first-order oscillation probability $P(\nu_\mu \to \nu_e)$ calculated in Sects. 5.1 and Appendix D.1. We can identify the following "clustering variables" at the level of the $\widetilde{S}^{(1)}_{\rm EV}$ matrix elements:

$$K_{12}e^{-i\delta} + K_{21}e^{i\delta}, \qquad c_\varphi^2 K_{13} - c_\varphi s_\varphi K_{23}e^{i\delta}, \qquad c_\varphi s_\varphi K_{13} + c_\varphi^2 K_{23}e^{i\delta}, \tag{66}$$

where we have not listed $(s_\varphi^2 K_{13} + c_\varphi s_\varphi K_{23}e^{i\delta})$ and $(c_\varphi s_\varphi K_{13} - s_\varphi^2 K_{23}e^{i\delta})$. They are not dynamically independent from the ones in Eq. (66) because they can be generated by the symmetry transformation (61) from the second and the third in Eq. (66). Also there exists the exceptional, isolated one $K_{12}e^{-i\delta}$ in Eq. (D2).

In Eq. (66), we did not quote the diagonal variables which come as a form of the difference, for example $(K_{22} - K_{11})$, because these combinations are enforced by rephasing invariance. However, these diagonal α parameter differences often come in a particular combination with the other cluster variables, e.g., as $\left[\cos 2\varphi\,(K_{22} - K_{11}) + \sin 2\varphi\left(K_{12}e^{-i\delta} + K_{21}e^{i\delta}\right)\right]$,

[17] To close a possible loophole in this statement, we performed an explicit construction of the solar resonance perturbation theory extended with the UV effect using the ATM convention of $U_{\rm MNS}$. A preliminary investigation reveals that the same δ–(cluster of the α parameters) correlation as in Eq. (65) survives, but inside $K_{ij}\,\widetilde{\alpha}_{\beta\gamma}$ must be transformed to $\alpha_{\beta\gamma}$ (α matrix elements in the ATM convention) by the transformation rule (13). This is the expected result and apparently there is no loophole in our prescription.

or $\left[\sin 2\varphi\,(K_{22}-K_{11})-\cos 2\varphi\left(K_{12}e^{-i\delta}+K_{21}e^{i\delta}\right)\right]$. Moreover, the other blobs of variables $\left(c_{13}^2K_{13}-s_{13}^2K_{31}\right)$, and $\left(c_{13}^2K_{23}e^{i\delta}-s_{13}^2K_{32}e^{-i\delta}\right)$, which are not visible at the level of the $\widetilde{S}^{(1)}_{\rm EV}$ matrix, shows up in the oscillation probability. See Eqs. (59) and (D2) - (D4) for all the above examples of blobs.

It seems that the appearance of such cluster variables as well as the correlation between δ and the α parameter blobs are worth some attention though we do not quite understand the cause of this phenomenon.

7. Physics of neutrino flavor transformation with non-unitary mixing matrix

Up to this section, we have aimed at analytical understanding of the system around the region of solar-scale enhanced oscillation; the "solar region", for short. Likewise, we use below the simplified terminology "atmospheric region" for a region of enhanced atmospheric-scale oscillation. Now, we discuss the physics of neutrino flavor transformation in the solar region. However, we do it in comparison with that of the atmospheric region as it proves to be more revealing. We try to illuminate some new aspects of the system of the three-flavor active neutrinos with non-unitary mixing matrix by using the numerical method together with our first-order formula.

We use the PDG convention of $U_{\rm MNS}$ in all the computations in this section, because it is used in most of the analyses of neutrino flavor transformations. We also depart from our "official" notations $\bar{\alpha}_{\beta\gamma}$ of the α parameters in the PDG convention defined in Sect. 4.1, and simply denote them as $\alpha_{\beta\gamma}$ in this section beyond the next subsection.

7.1. Use of the exact and perturbative oscillation probabilities: General convention of U_{MNS}

Towards the goal, we utilize the perturbative oscillation probability derived in Sect. 5, as well as the exact formula for the probability based on numerical integration of the evolution equation, the latter of which is valid even for a varied matter density.[18]

It was pointed out in Ref. [38] that the α matrix depends on the convention of $U_{\rm MNS}$. By using this property, one can derive a probability formula in the PDG or ATM conventions using the substitution rule from the $\widetilde{\alpha}$ parameter in the SOL convention to the $\bar{\alpha}$ parameter in the PDG, or the α parameter in the ATM conventions. See Eq. (13) in Sect. 4.1. One can also transform to a general $U_{\rm MNS}$ convention by using the phase redefinition $U(\beta,\gamma)$ defined in Ref. [38]. Notice that the translation rule applies not only in the perturbative formulas but also in the exact formulas.

7.2. Overview of the effect of UV

The first step to understand the effect of non-unitarity which is brought into the νSM three neutrino system by introducing the α matrix is to know where and how strongly the UV α parameters affect the neutrino flavor transformation. For this purpose, we turn on each $\alpha_{\beta\gamma}$ parameter one by one and calculate the non-unitary contribution to the appearance probability $\Delta P_{\mu e}$ defined by

$$\Delta P_{\mu e}\equiv P(\nu_\mu\to\nu_e)-P(\nu_\mu\to\nu_e)_{\nu\rm SM}=P(\nu_\mu\to\nu_e)_{\rm EV}+P(\nu_\mu\to\nu_e)_{\rm UV}, \tag{67}$$

[18] If the uniform matter density approximation applies one can also use the exact analytic formula for the probability derived in Ref. [25]. We note that the expression is reasonably simple despite its exactitude.

where $P(\nu_\mu \to \nu_e)$ in Eq. (67) denotes the appearance probability in the $\nu_\mu \to \nu_e$ channel with the UV effect fully implemented. Both $P(\nu_\mu \to \nu_e)$ and $P(\nu_\mu \to \nu_e)_{\nu\text{SM}}$ are computed numerically. In all the calculations in this section, the matter density is taken to be $\rho = 3.2$ g cm^{-3} over the entire baseline.

In Fig. 1 we show $\Delta P_{\mu e}$ by using color grading guided by the contour lines. In each panel we turn on one of $\alpha_{\beta\gamma}$, from the top left-hand to the bottom right-hand panels, in order: α_{ee}, $\alpha_{\mu\mu}$, $\alpha_{\tau\tau}$, $\alpha_{\mu e}$, $\alpha_{\tau e}$, and $\alpha_{\tau\mu}$.[19] In this section, we turn on only one of the $\alpha_{\beta\gamma}$ parameters in each panel, except for the top right-hand and bottom two panels in Fig. 2. To have an insight into the required accuracy of the $P(\nu_\mu \to \nu_e)$ measurement to improve the current bounds by a factor of 2, we take the value of each $\alpha_{\beta\gamma}$ as half of the bound obtained by Blennow et al. [26] with the positive sign. Figure 1 as a whole displays how large the UV effect is depending upon the energy E and the baseline L. The "mountain ridges" roughly follow the line of $L/E =$ constant. The atmospheric and the solar MSW enhancements are visible, respectively, at around $E \sim 10$ GeV and near the upper end of $L = 10^4$ km, and $E \simeq$ several $\times 100$ MeV and $E \simeq$ several $\times 1000$ km.

We observe two salient features:

- $\Delta P_{\mu e}$ is at most $\simeq \pm 1\%$ in all the panels in Fig. 1, which means a 1% level measurement of the probability is necessary for a factor of 2 improvement of the bounds.
- $\Delta P_{\mu e}$ changes sign depending upon which $\alpha_{\beta\gamma}$ is turned on, and on the region of kinematical phase space, e.g., in the atmospheric region, or the solar region.

The 1% accuracy measurement of the probability is mentioned at the end of Sect. 4.2 in relation to the possible target accuracy of constraining UV α parameters.

For the second point above, we notice in Fig. 1 that with turning on $\alpha_{\tau\tau}$ (middle left-hand panel) $\Delta P_{\mu e}$ is positive in the solar region and negative in the atmospheric region. On the other hand, this tendency is reversed completely with $\alpha_{\tau e}$ (bottom left-hand panel), and less completely with $\alpha_{\mu e}$ (middle right-hand panel). In the other cases, $\Delta P_{\mu e}$ is negative in both the regions of the atmospheric-scale and solar-scale enhancement. This means that if we turn on all $\alpha_{\beta\gamma}$ at once, the effect of each element may cancel each other at least partly. One must also take into account the fact that, since we do not know a priori the sign of the α parameters, the pattern of the cancellation can be more complicated when all the parameters are turned on with arbitrary signs, or if phases are attached to the off-diagonal α parameters. This implies that (1) determination of the UV $\alpha_{\beta\gamma}$ parameters (assuming their existence) could have additional difficulties due to confusion and degeneracy caused by the cancellation between the effect of different α parameters, and (2) the bound on UV obtained by using the "one $\alpha_{\beta\gamma}$ turned on at one time" procedure could have made the bound artificially stronger than the one obtained with the proper procedure of "all $\alpha_{\beta\gamma}$ turned on but the rest of them marginalized".

The features of possible cancellation between the effect of $\alpha_{\beta\gamma}$ parameters may add another difficulty to the task of identifying their effects, an already highly non-trivial one due to high pre-

[19] Notice that if the diagonal α parameters enter into the probability in the form $\alpha_{\beta\beta} - \alpha_{\gamma\gamma}$, only two of the three diagonal α parameters are independent. However, since this subtractive dependence holds only in the first order in UV expansion [38], the independent bounds exist for all three of them. This is in sharp contrast to the situation for the NSI parameters.

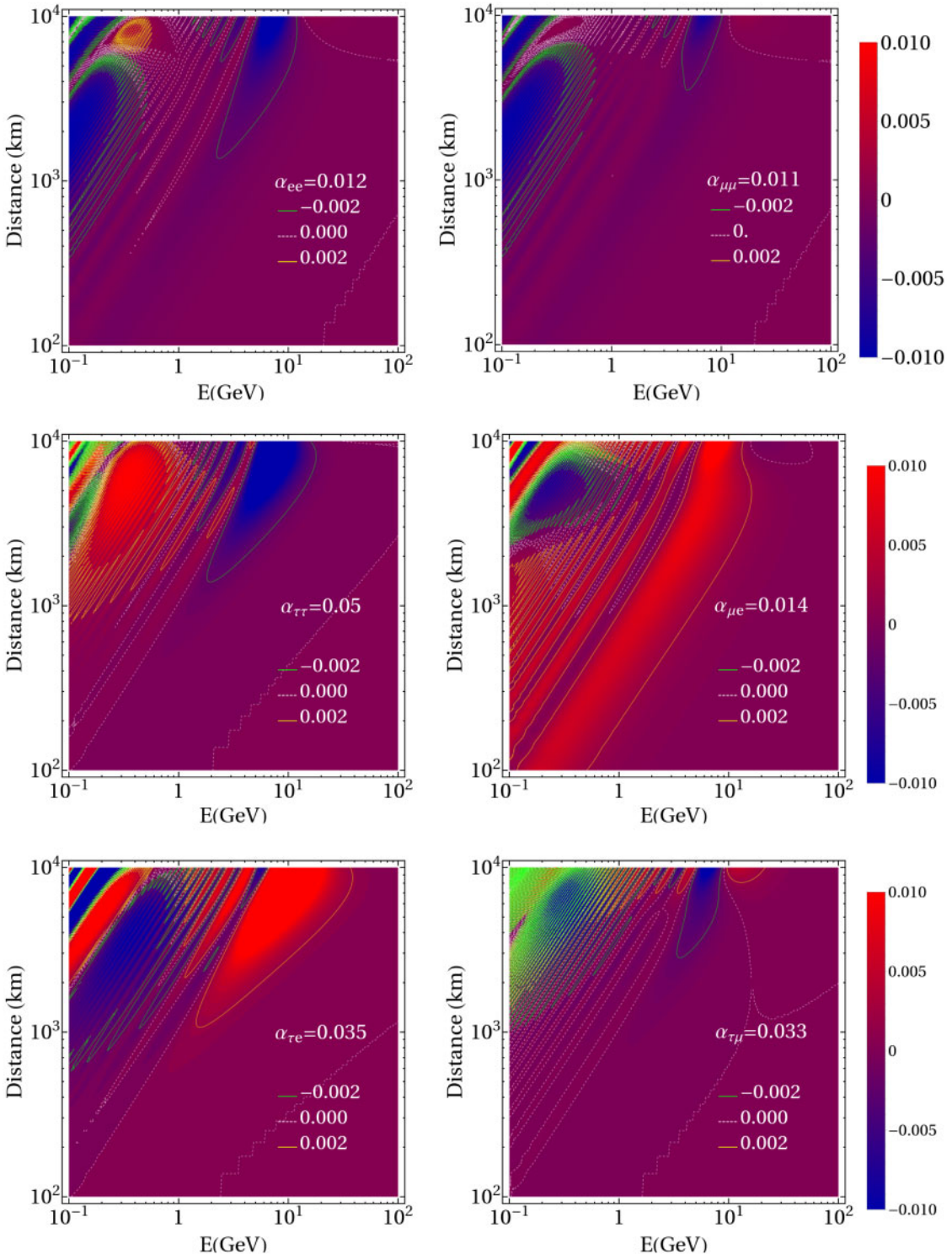

Fig. 1. Plotted is $\Delta P_{\mu e} \equiv P(\nu_\mu \to \nu_e) - P(\nu_\mu \to \nu_e)_{\nu\text{SM}}$ by turning on one $\alpha_{\beta\gamma}$ at a time, in order from the top left-hand to the bottom right-hand panels, α_{ee}, $\alpha_{\mu\mu}$, $\alpha_{\tau\tau}$, $\alpha_{\mu e}$, $\alpha_{\tau e}$, and $\alpha_{\tau\mu}$. We take the value of each $\alpha_{\beta\gamma}$ as half of the bound obtained by Blennow et al. [26] given in Table 2 in Appendix A: $\alpha_{ee} = 0.012$, $\alpha_{\mu\mu} = 0.011$, $\alpha_{\tau\tau} = 0.05$, $\alpha_{\mu e} = 0.014$, $\alpha_{\tau e} = 0.035$, and $\alpha_{\tau\mu} = 0.033$. The matter density is taken to be $\rho = 3.2$ g cm^{-3} over the entire baseline.

cision required to measure the probability. Therefore, further discussion of the question of how to disentangle the effects of different alpha parameters is called for.

7.3. *Unitary vs. non-unitary pieces of the UV related oscillation probability*

The UV α parameter related part of the probability $\Delta P_{\mu e}$ decomposes into two parts, the unitary evolution part $P(\nu_\mu \to \nu_e)_{\rm EV}$ and the genuine non-unitary part $P(\nu_\mu \to \nu_e)_{\rm UV}$ [38]; see Eq. (55). Then, a natural question is which part is larger or dominating, and whether they mutually tend to add up or cancel each other out.

These questions are answered by Fig. 2. In the top two panels the whole UV effects, $\Delta P_{\mu e} = P(\nu_\mu \to \nu_e)_{\rm UV} + P(\nu_\mu \to \nu_e)_{\rm EV}$ are presented, with $\alpha_{\mu e} = 0.014$ only in the left-hand panel, and with $\alpha_{ee} = 0.012$ and $\alpha_{\mu\mu} = 0.011$ in the right-hand panel. The values of the α parameters are the same as used in Fig. 1, and hence the left-hand panel overlaps with a part of the middle-right-hand panel of Fig. 1.

The decomposition of $\Delta P_{\mu e}$ into $P(\nu_\mu \to \nu_e)_{\rm UV}$ and $P(\nu_\mu \to \nu_e)_{\rm EV}$ is displayed in the middle ($\alpha_{\mu e} = 0.014$ case) and bottom ($\alpha_{ee} = 0.012$ and $\alpha_{\mu\mu} = 0.011$ case) panels of Fig. 2, respectively. We restrict ourselves into the two choices of the α parameters because $P(\nu_\mu \to \nu_e)_{\rm UV}$ in the first order depends only on the two combinations $\alpha_{\mu e}$ and $\alpha_{ee} + \alpha_{\mu\mu}$. $P(\nu_\mu \to \nu_e)_{\rm EV}$ is computed by using the formula $P(\nu_\mu \to \nu_e) - P(\nu_\mu \to \nu_e)_{\nu\rm SM} - P(\nu_\mu \to \nu_e)^{(1)}_{\rm UV}$ with the first-order expression of $P(\nu_\mu \to \nu_e)_{\rm UV}$, and hence $P(\nu_\mu \to \nu_e)_{\rm EV}$ is accurate only to the first order.

An overall feature is that in wide areas in Fig. 2 $P(\nu_\mu \to \nu_e)_{\rm UV}$ and $P(\nu_\mu \to \nu_e)_{\rm EV}$ tend to cancel each other out. In looking into the figure more closely, however, we observe a little more intricate features. In the $\alpha_{\mu e} = 0.014$ case (middle panels), above the $L/E = 10^4$ km/230 MeV line, $P(\nu_\mu \to \nu_e)_{\rm UV}$ contributes to lift up the probability, enhancing the yellow regions of $P(\nu_\mu \to \nu_e)_{\rm EV}$ into the thicker ones in $\Delta P_{\mu e}$. Below the line, $P(\nu_\mu \to \nu_e)_{\rm UV}$ is more dominating in the blue solar resonance region, but is partially cancelled by $P(\nu_\mu \to \nu_e)_{\rm EV}$. The cancellation is even more prominent in the bottom panels, the case with $\alpha_{ee} + \alpha_{\mu\mu}$ turned on. The overall feature of the color-graded contour of $\Delta P_{\mu e}$ is similar to that of $P(\nu_\mu \to \nu_e)_{\rm UV}$, but $P(\nu_\mu \to \nu_e)_{\rm EV}$ over-cancels the peaks of $P(\nu_\mu \to \nu_e)_{\rm UV}$ above the $L/E = 10^4$ km/230 MeV line.

This feature of cancellation is akin to, but is much more prominent compared to, that observed in the "atmospheric region" in Ref. [38]. Unfortunately, we cannot offer a physical explanation as to why the cancellation between $P(\nu_\mu \to \nu_e)_{\rm UV}$ and $P(\nu_\mu \to \nu_e)_{\rm EV}$ takes place, or why the feature is common to both the atmospheric and the solar regions. In most of the regions it acts as a partial "hiding mechanism" of non-unitarity since a less prominent effect is left in the observable, the appearance probability $P(\nu_\mu \to \nu_e)$. To obtain the information of the genuine non-unitary part $P(\nu_\mu \to \nu_e)_{\rm UV}$, it must be complemented by measurement of departure from unitarity, $P(\nu_\mu \to \nu_e) + P(\nu_\mu \to \nu_\mu) + P(\nu_\mu \to \nu_\tau) \neq 1$.

7.4. *νSM–α parameter phase correlation: The atmospheric vs. solar regions*

We have learned in the previous section that the features of the parameter correlation between the νSM and the UV new physics parameters in the solar region is different from the ones in the atmospheric region. A new δ–(blobs of the α parameters) correlation is observed. Then, it is natural to ask the question: What is the feature of νSM–UV parameter CP phase correlation in the solar region, and which characteristic difference does it have from those in the atmospheric region?

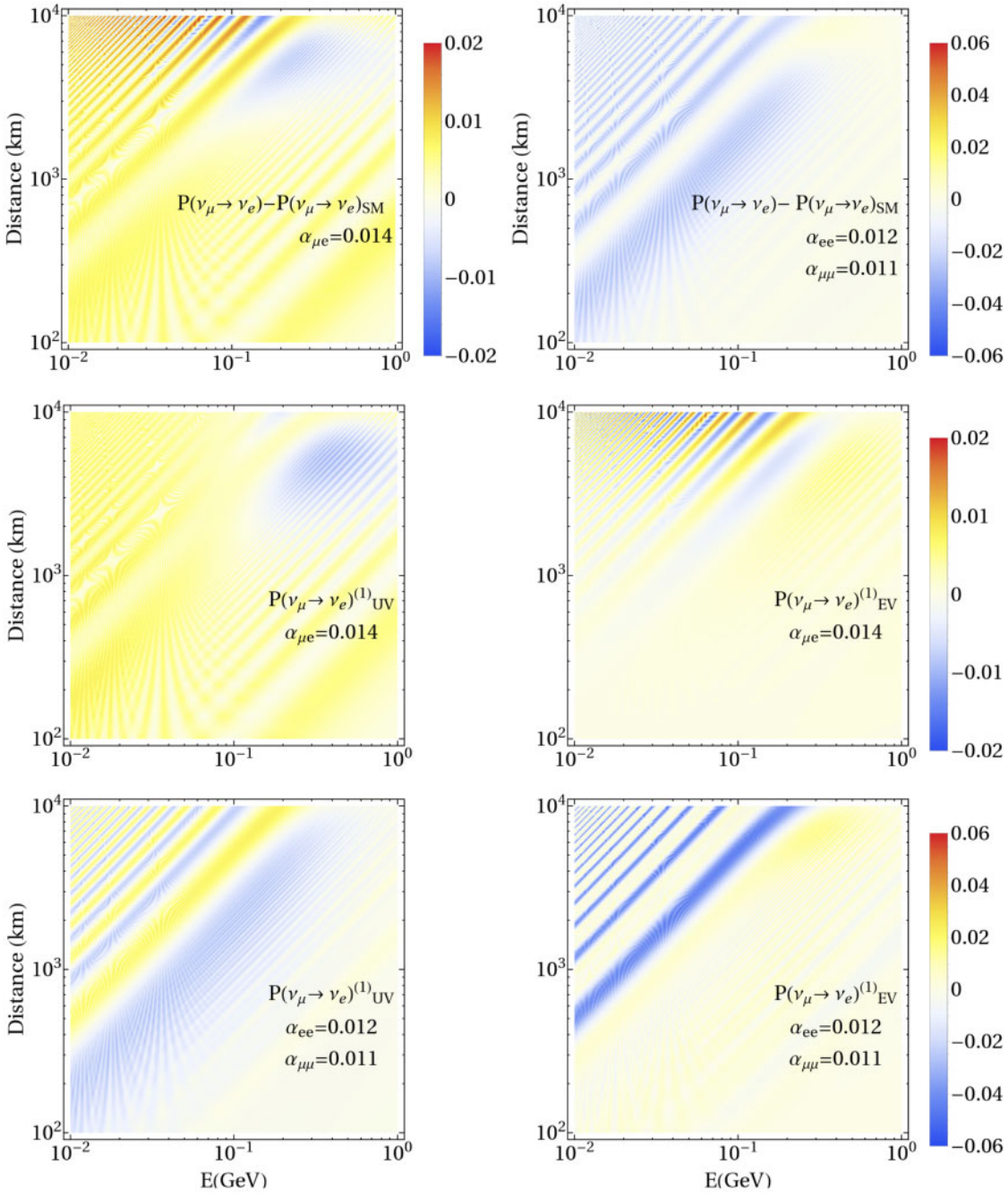

Fig. 2. In the top two panels, $\Delta P_{\mu e} = P(\nu_\mu \to \nu_e)_{\rm UV} + P(\nu_\mu \to \nu_e)_{\rm EV}$ are presented by the color grading, with $\alpha_{\mu e} = 0.014$ (left-hand panel), and with $\alpha_{ee} = 0.012$ and $\alpha_{\mu\mu} = 0.011$ (right-hand panel). In the middle and bottom panels, $\Delta P_{\mu e}$ is decomposed to $P(\nu_\mu \to \nu_e)_{\rm UV}$ and $P(\nu_\mu \to \nu_e)_{\rm EV}$ in the left- and right-hand panels, respectively.

To discuss correlation between δ and phases of the off-diagonal α parameters, we parametrize the latter as

$$\alpha_{\beta\gamma} = |\alpha_{\beta\gamma}| e^{i\phi_{\beta\gamma}}, \tag{68}$$

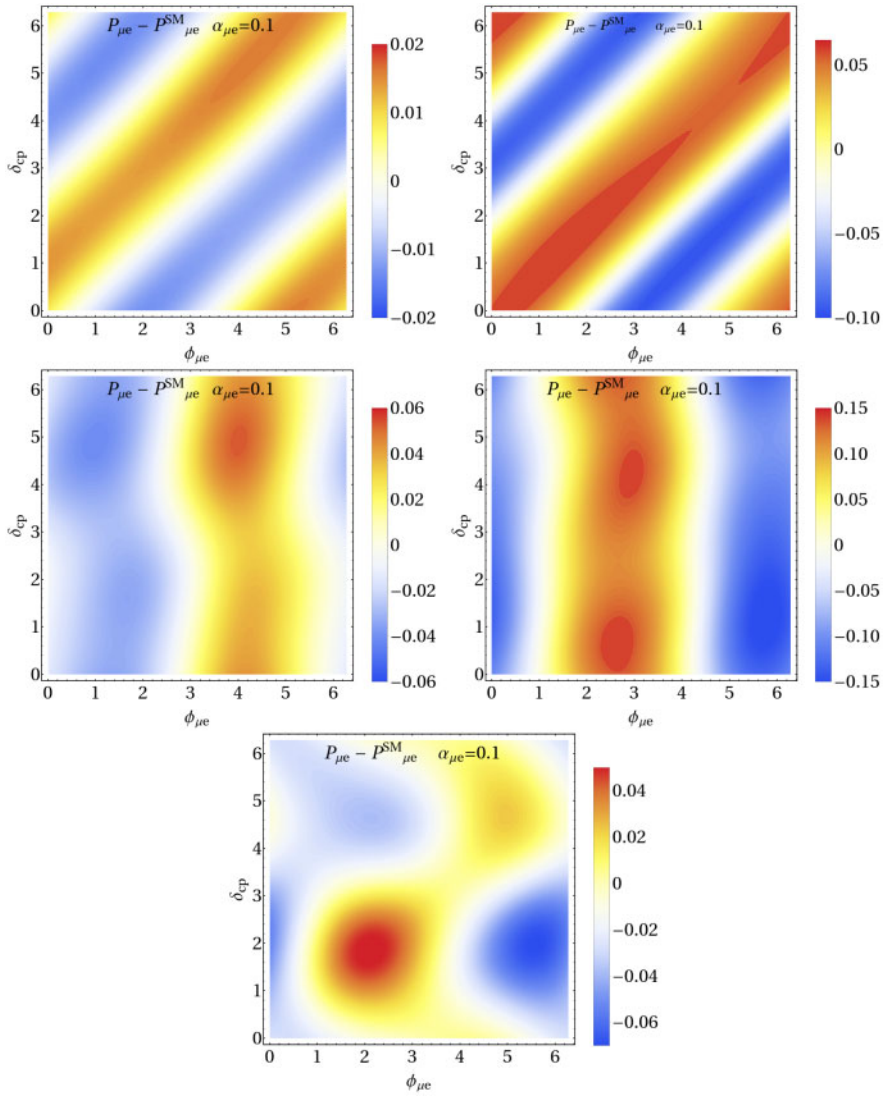

Fig. 3. $\Delta P_{\mu e} \equiv P(\nu_\mu \to \nu_e) - P(\nu_\mu \to \nu_e)_{\nu\text{SM}}$ is presented in the $\phi_{\mu e}$–δ plane by color graduation, which is calculated by turning on $\alpha_{\mu e} = 0.1$ only. The top two panels are in the atmospheric region with energy $E = 10$ GeV, and the middle two panels are in the solar region with energy $E = 200$ MeV. The baseline is taken as $L = 3000$ km (left-hand panel) and $L = 12000$ km (right-hand panel), in both the top and middle panels. The bottom panel is in the solar region with $E = 300$ MeV and $L = 5000$ km.

where $\beta\gamma = \mu e, \tau e, \tau\mu$. To make the phase correlation clearly visible, we use $\Delta P_{\mu e} \equiv P(\nu_\mu \to \nu_e) - P(\nu_\mu \to \nu_e)_{\nu\text{SM}}$ defined in Eq. (67), not the probability itself.

In Fig. 3, the non-unitary contribution to the appearance probability $\Delta P_{\mu e}$ computed by turning on $\alpha_{\mu e}$ only is presented on the $\phi_{\mu e}$–δ plane by showing the equi-contours of $\Delta P_{\mu e}$ with color grading. In Figs. 4 and 5, the results of the similar exercises are presented, the case with $\alpha_{\tau e}$ turned on (Fig. 4), and the one with $\alpha_{\tau\mu}$ (Fig. 5). In Figs. 3, 4, and 5, we use a large value $\alpha_{\beta\gamma} = 0.1$ to enhance effects of the phase correlation, which merits higher visibility. The global features of the δ–α parameter phase correlation shown in Figs. 3, 4 and 5 are:

- The linear, oblique correlation seen in the case of both $\alpha_{\mu e} \neq 0$ (Fig. 3) and $\alpha_{\tau e} \neq 0$ (Fig. 4) in the atmospheric region shown in the upper panels, but no clearly visible correlation in any of the other panels.

- The absolute value of $|\Delta P_{\mu e}|$ is larger in the panels with baseline $L = 12000$ km than those with $L = 3000$ km by a factor of ~ 5. This statement applies to all the panels including both the atmospheric and solar regions.

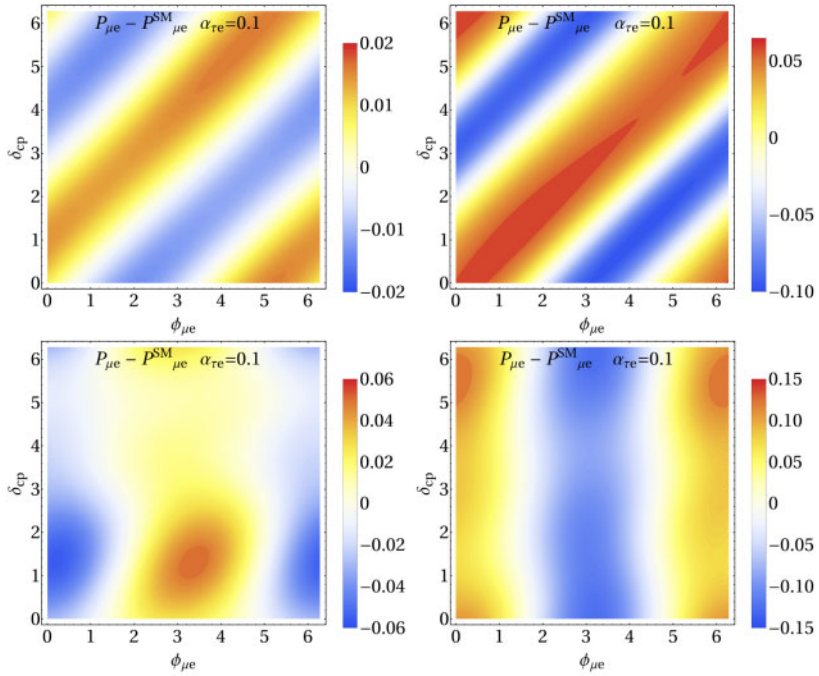

Fig. 4. $\Delta P_{\mu e} \equiv P(\nu_\mu \to \nu_e) - P(\nu_\mu \to \nu_e)_{\nu\rm SM}$ is presented in the $\phi_{\mu e}$–δ plane by color graduation, which is calculated by turning on $\alpha_{\tau e} = 0.1$ only. The upper two panels are in the atmospheric region with energy $E = 10$ GeV, and the lower two panels are in the solar region with energy $E = 200$ MeV. The baseline is taken as $L = 3000$ km (left-hand panel) and $L = 12000$ km (right-hand panel), in both the upper and lower panels.

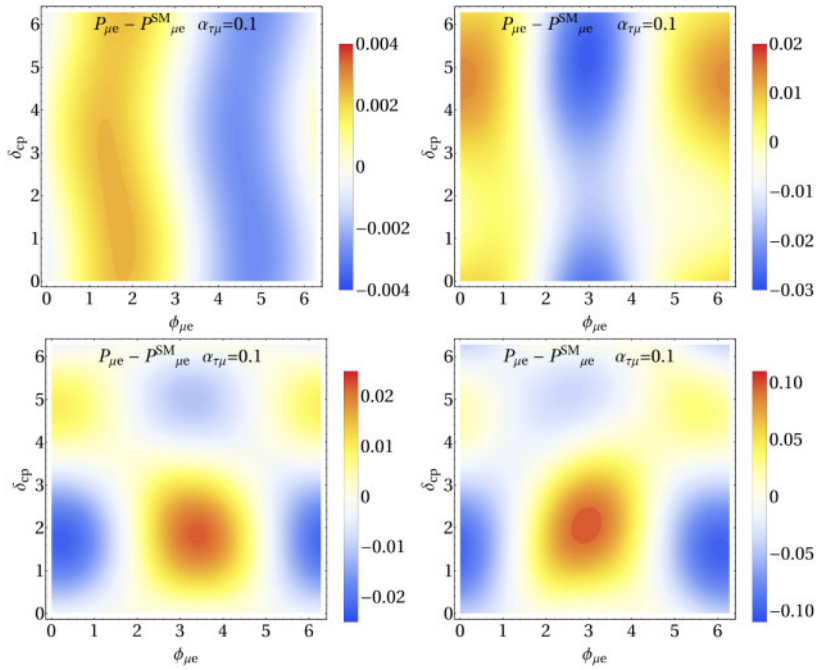

Fig. 5. The same as in Fig. 4 but with only $\alpha_{\tau\mu} = 0.1$ turned on.

Let us start from a discussion of the phase correlation seen in the atmospheric region—the top two panels in Figs. 3, 4 and 5. The linear, oblique correlations seen in Figs. 3 and 4, $\phi_{\mu e}$–δ and $\phi_{\tau e}$–δ correlations, respectively, and the lack of visible correlation between $\phi_{\tau\mu}$ and δ shown in Fig. 5 (all in the upper two panels) is perfectly consistent with the "canonical phase combination" [38][20]

$$e^{-i\delta}\alpha_{\mu e},\ \ e^{-i\delta}\alpha_{\tau e},\ \ \alpha_{\tau\mu}, \tag{69}$$

which holds under the PDG convention of $U_{\rm MNS}$. One should note the non-trivial $U_{\rm MNS}$ convention dependence: In the ATM phase convention of $U_{\rm MNS}$ (in which $e^{\pm i\delta}$ is attached to s_{23}), the phase correlation takes the form $[e^{-i\delta}\alpha_{\mu e}, \alpha_{\tau e}, e^{i\delta}\alpha_{\tau\mu}]$ [38].

On the other hand, the features of the phase correlation in the solar region shown in the lower panels in Figs. 3, 4 and 5 are more subtle and not easy to understand. In some panels, the equal-$\Delta P_{\mu e}$ contours are vertical, which may imply that there is no significant correlation between δ and α parameter phases. In the other, there exists "circular-shaped correlation" with positive and negative signs of $\Delta P_{\mu e}$ in the two-dimensional phase space. Notice that in the panels with vertical correlation and with "circular correlation", the δ (in-)dependence cannot be understood as a remnant of insufficient subtraction of the νSM part. This is because the values of $\Delta P_{\mu e}$ and its variation in ϕ or δ directions can be as large as ~ 0.1, of the order of the α parameter that is turned on. The feature of the ϕ–δ phase correlation, in particular, the coexistence of the vertical and circular shaped correlations is not understood, regrettably, by our analytic framework.[21]

With regard to the baseline dependence of the strength of the correlation, it might be that $|\Delta P_{\mu e}|$ itself is larger at the longer baseline of $L = 12000$ km among the two baselines we have chosen to display in Figs. 3, 4 and 5.

The features of the α parameter phase–νSM δ correlation in the atmospheric and the solar regions presented in Figs. 3, 4 and 5 testify that the nature of the correlation is quite dynamical, confirming our view stated in Sect. 3. Unfortunately, physical understanding of the features of the phase correlation in the solar region are not yet achieved, which calls for further studies.

8. Concluding remarks

In this paper, we have attempted to achieve an understanding of the physics of the three-flavor neutrino system with non-unitary mixing matrix. We have focused our discussion on elucidating the nature of parameter correlations in such a system, in particular the correlation between the νSM and the UV new physics parameters. We do this in the region of the solar-scale oscillations, the "solar

[20] If the probability calculated by first-order helio-UV perturbation theory [38] is sufficiently accurate, there should be no δ dependence in the upper two panels in Fig. 5, because the δ dependence would have been eliminated by the subtraction of $P(\nu_\mu \to \nu_e)_{\nu\rm SM}$. Obviously, this is not the case. Notice that the results presented in Figs. 3, 4 and 5 are accurate as they do not rely on perturbative treatment. This means that the perturbative treatment fails to provide accurate description of the probability, which is natural due to the large value of 0.1 taken for $\alpha_{\tau\mu}$. In fact, the remaining δ dependence is up to a few $\times 10^{-3}$ level for $L = 3000$ km, and is of the order $\sim \pm 0.02$ for $L = 12000$ km, so that our interpretation may be valid.

[21] It appears that there are some regularities which may be relevant for understanding the phase correlation in the solar region. That is, we often observe "red" ($\Delta P_{\mu e} > 0$) and "blue" ($\Delta P_{\mu e} < 0$) vertical contours in central region, $\phi \sim \pi$. It is likely that the central "red" vertical correlation corresponds to the region of negative $\Delta P_{\mu e}$ in Fig. 1, whereas the central "blue" vertical correlation corresponds to the region of positive $\Delta P_{\mu e}$ in Fig. 1. For the latter, we refer to the lower right-hand panel of Fig. 4, and the case of $\alpha_{\tau e} = 0.1$, $E = 200$ MeV and $L = 5000$ km.

region" for short, in this paper. It nicely complements the one given in our previous paper [38] which dealt with the region of atmospheric-scale oscillations, the "atmospheric region".

Towards this goal, we have formulated a new perturbative framework to discuss effect of a non-unitary mixing matrix in the solar region, the UV extended version of the "solar-resonance perturbation theory" [41]. It was necessary to resolve the question raised in Ref. [38] which casts doubt on the physical reality of the correlation between the νSM δ and the phases of UV α parameters. However, in turn, the framework serves as a powerful analytic machinery for analyzing the features of parameter correlation in the solar region. The skepticism about the reality of the phase correlation, which is described in detail in Sect. 1, is cleared up by showing that the phase correlation *does exist* in the solar region with the SOL ($e^{\pm i\delta}$ attached to s_{12}) convention of U_{MNS}. See Sect. 6.

In fact, we have uncovered that the features of the νSM–UV parameter correlations are much more profound than we thought. This point can be illuminated most clearly by contrasting the atmospheric region to the solar one. In the atmospheric region, the most notable feature is the νSM δ–UV α parameter phase correlation of the "chiral type", $[e^{-i\delta}\alpha_{\mu e}, e^{-i\delta}\alpha_{\tau e}, \alpha_{\tau\mu}]$ in the PDG convention of U_{MNS} [38]. This picture no longer holds in the solar region, and the correlation takes the form of δ–(blobs of the α parameters) correlation as we saw in Sect. 6.2. Another interesting observation in this context is that when we move the kinematical region from $E/L = 200$ MeV/3000 km to $E/L = 300$ MeV/5000 km, the δ–$\phi_{\mu e}$ correlation takes vastly different forms, as shown in Fig. 3, where $\phi_{\mu e}$ denotes the phase of $\alpha_{\mu e}$.

We have utilized the analytic framework developed in this paper as well as the numerical method to reveal more generic features of the effects of the UV α parameters. In addition to the ones mentioned above, we have observed that the effect of non-unitarity tends to cancel between the unitary evolution part (denoted as "EV") and the non-unitary part (denoted as "UV") of the probability, and between the different $\alpha_{\beta\gamma}$ parameters. see Sect. 7.

One of the most intriguing features of the parameter correlation is that the form of the correlation depends also on the values of the mixing parameters. The phenomenon is briefly mentioned in Sect. 3.2; as θ_{13} becomes larger, the correlation seen at smaller θ_{13} starts to dissolve. Since we cannot control the values of the mixing angles or Δm^2 by ourselves, the discussion might look appealing only to an academic interest. However, we believe that it merits deepening our understanding on the mechanism and the cause of parameter correlation. We are not able to explore this point further in this paper, and a focused investigation on this issue is called for.

All these features of the parameter correlation may be summarized by the term *"dynamical nature of the parameter correlation"*.

Finally, we remark that the occurrence of dynamical correlations between the parameters in systems with many degrees of freedom is very common, as discussed in Sect. 3. The rich variety of correlations we encountered in our system with non-unitarity adds another example to this list. If one chooses the way of testing leptonic unitarity by setting up a class of models with UV and confrontation of them with experimental data, understanding the system with UV would be an indispensable step in carrying out this task. Yet we must emphasize that our understanding of the system, e.g., of the parameter correlation, is far from sufficient, generically in the system with new physics beyond the νSM.

On the experimental side, if we want to utilize the low-energy region with the solar-scale enhanced oscillation, in the context of the *precision* unitarity test, a possible advantage of the Kamioka–Korea identical two-detector setup [16,67] may be worth renewed attention. Fortunately, the construction of Hyper-K has been started, which may act as the Kamioka site detector in an extended plan of the two-detector complex [15,49].

Acknowledgements

One of the authors (I.M.S.) acknowledges travel support from the Colegio de Física Fundamental e Interdisciplinaria de las Américas (COFI). Fermilab is operated by the Fermi Research Alliance, LLC under contract No. DE-AC02-07CH11359 with the United States Department of Energy. The other (H.M.) thanks Center for Neutrino Physics, Department of Physics, Virginia Tech for hospitality and support.

Funding

Open Access funding: SCOAP[3].

Appendix A. Explicit expressions of F_{ij}, K_{ij} and Φ_{ij}

The explicit expressions of the elements F_{ij}, K_{ij} and Φ_{ij} defined, respectively, in Eqs. (22), (23) and (45) are given as follows:

$$
\begin{aligned}
F_{11} &= 2\widetilde{\alpha}_{ee}\left(1-\frac{\Delta_a}{\Delta_b}\right),\\
F_{12} &= c_{23}\widetilde{\alpha}^*_{\mu e} - s_{23}\widetilde{\alpha}^*_{\tau e},\\
F_{13} &= s_{23}\widetilde{\alpha}^*_{\mu e} + c_{23}\widetilde{\alpha}^*_{\tau e},\\
F_{21} &= c_{23}\widetilde{\alpha}_{\mu e} - s_{23}\widetilde{\alpha}_{\tau e} = (F_{12})^*\\
F_{22} &= 2\left[c^2_{23}\widetilde{\alpha}_{\mu\mu} + s^2_{23}\widetilde{\alpha}_{\tau\tau} - c_{23}s_{23}\mathrm{Re}\left(\widetilde{\alpha}_{\tau\mu}\right)\right],\\
F_{23} &= \left[2c_{23}s_{23}(\widetilde{\alpha}_{\mu\mu} - \widetilde{\alpha}_{\tau\tau}) + c^2_{23}\widetilde{\alpha}^*_{\tau\mu} - s^2_{23}\widetilde{\alpha}_{\tau\mu}\right],\\
F_{31} &= s_{23}\widetilde{\alpha}_{\mu e} + c_{23}\widetilde{\alpha}_{\tau e} = (F_{13})^*,\\
F_{32} &= \left[2c_{23}s_{23}(\widetilde{\alpha}_{\mu\mu} - \widetilde{\alpha}_{\tau\tau}) + c^2_{23}\widetilde{\alpha}_{\tau\mu} - s^2_{23}\widetilde{\alpha}^*_{\tau\mu}\right] = (F_{23})^*,\\
F_{33} &= 2\left[s^2_{23}\widetilde{\alpha}_{\mu\mu} + c^2_{23}\widetilde{\alpha}_{\tau\tau} + c_{23}s_{23}\mathrm{Re}\left(\widetilde{\alpha}_{\tau\mu}\right)\right].
\end{aligned}
\tag{A1}
$$

$$
\begin{aligned}
K_{11} &= 2c^2_{13}\widetilde{\alpha}_{ee}\left(1-\frac{\Delta_a}{\Delta_b}\right) + 2s^2_{13}\left[s^2_{23}\widetilde{\alpha}_{\mu\mu} + c^2_{23}\widetilde{\alpha}_{\tau\tau} + c_{23}s_{23}\mathrm{Re}\left(\widetilde{\alpha}_{\tau\mu}\right)\right],\\
&\quad - 2c_{13}s_{13}\mathrm{Re}\left(s_{23}\widetilde{\alpha}_{\mu e} + c_{23}\widetilde{\alpha}_{\tau e}\right)\\
K_{12} &= c_{13}\left(c_{23}\widetilde{\alpha}^*_{\mu e} - s_{23}\widetilde{\alpha}^*_{\tau e}\right) - s_{13}\left[2c_{23}s_{23}(\widetilde{\alpha}_{\mu\mu} - \widetilde{\alpha}_{\tau\tau}) + c^2_{23}\widetilde{\alpha}_{\tau\mu} - s^2_{23}\widetilde{\alpha}^*_{\tau\mu}\right] = (K_{21})^*,\\
K_{13} &= 2c_{13}s_{13}\left[\widetilde{\alpha}_{ee}\left(1-\frac{\Delta_a}{\Delta_b}\right) - \left(s^2_{23}\widetilde{\alpha}_{\mu\mu} + c^2_{23}\widetilde{\alpha}_{\tau\tau}\right)\right]\\
&\quad + c^2_{13}\left(s_{23}\widetilde{\alpha}^*_{\mu e} + c_{23}\widetilde{\alpha}^*_{\tau e}\right) - s^2_{13}\left(s_{23}\widetilde{\alpha}_{\mu e} + c_{23}\widetilde{\alpha}_{\tau e}\right) - 2c_{23}s_{23}c_{13}s_{13}\mathrm{Re}\left(\widetilde{\alpha}_{\tau\mu}\right) = (K_{31})^*,\\
K_{22} &= 2\left[c^2_{23}\widetilde{\alpha}_{\mu\mu} + s^2_{23}\widetilde{\alpha}_{\tau\tau} - c_{23}s_{23}\mathrm{Re}\left(\widetilde{\alpha}_{\tau\mu}\right)\right],\\
K_{23} &= s_{13}\left(c_{23}\widetilde{\alpha}_{\mu e} - s_{23}\widetilde{\alpha}_{\tau e}\right) + c_{13}\left[2c_{23}s_{23}(\widetilde{\alpha}_{\mu\mu} - \widetilde{\alpha}_{\tau\tau}) + c^2_{23}\widetilde{\alpha}^*_{\tau\mu} - s^2_{23}\widetilde{\alpha}_{\tau\mu}\right] = (K_{32})^*,\\
K_{33} &= 2s^2_{13}\widetilde{\alpha}_{ee}\left(1-\frac{\Delta_a}{\Delta_b}\right) + 2c^2_{13}\left[s^2_{23}\widetilde{\alpha}_{\mu\mu} + c^2_{23}\widetilde{\alpha}_{\tau\tau} + c_{23}s_{23}\mathrm{Re}\left(\widetilde{\alpha}_{\tau\mu}\right)\right]
\end{aligned}
$$

$$+ 2c_{13}s_{13}\mathrm{Re}\left(s_{23}\widetilde{\alpha}_{\mu e} + c_{23}\widetilde{\alpha}_{\tau e}\right). \tag{A2}$$

$$\begin{aligned}
\Phi_{11} &= K_{11} + 2c_\varphi^2 s_\varphi^2 \left(K_{22} - K_{11}\right) - c_\varphi^2 s_\varphi^2 \left(K_{22} - K_{11}\right)\left\{e^{i(h_2-h_1)x} + e^{-i(h_2-h_1)x}\right\} \\
&\quad - c_\varphi s_\varphi \cos 2\varphi \left(K_{12}e^{-i\delta} + K_{21}e^{i\delta}\right) \\
&\quad + c_\varphi s_\varphi \left\{-\left(s_\varphi^2 K_{12}e^{-i\delta} - c_\varphi^2 K_{21}e^{i\delta}\right)e^{i(h_2-h_1)x} + \left(c_\varphi^2 K_{12}e^{-i\delta} - s_\varphi^2 K_{21}e^{i\delta}\right)e^{-i(h_2-h_1)x}\right\}, \\
\Phi_{12} &= e^{i\delta}\Bigg[c_\varphi s_\varphi \cos 2\varphi \left(K_{22} - K_{11}\right) + c_\varphi s_\varphi \left\{s_\varphi^2 e^{i(h_2-h_1)x} - c_\varphi^2 e^{-i(h_2-h_1)x}\right\}\left(K_{22} - K_{11}\right) \\
&\quad + 2c_\varphi^2 s_\varphi^2 \left(K_{12}e^{-i\delta} + K_{21}e^{i\delta}\right) + s_\varphi^2 \left(s_\varphi^2 K_{12}e^{-i\delta} - c_\varphi^2 K_{21}e^{i\delta}\right)e^{i(h_2-h_1)x} \\
&\quad + c_\varphi^2 \left(c_\varphi^2 K_{12}e^{-i\delta} - s_\varphi^2 K_{21}e^{i\delta}\right)e^{-i(h_2-h_1)x}\Bigg], \\
\Phi_{13} &= \left(s_\varphi^2 K_{13} + c_\varphi s_\varphi K_{23}e^{i\delta}\right)e^{-i(h_3-h_2)x} + \left(c_\varphi^2 K_{13} - c_\varphi s_\varphi K_{23}e^{i\delta}\right)e^{-i(h_3-h_1)x},
\end{aligned}$$

$$\begin{aligned}
\Phi_{21} &= e^{-i\delta}\Bigg\{c_\varphi s_\varphi \cos 2\varphi \left(K_{22} - K_{11}\right) - c_\varphi s_\varphi \left\{c_\varphi^2 e^{i(h_2-h_1)x} - s_\varphi^2 e^{-i(h_2-h_1)x}\right\}\left(K_{22} - K_{11}\right) \\
&\quad + 2c_\varphi^2 s_\varphi^2 \left(K_{12}e^{-i\delta} + K_{21}e^{i\delta}\right) + c_\varphi^2 \left(c_\varphi^2 K_{21}e^{i\delta} - s_\varphi^2 K_{12}e^{-i\delta}\right)e^{i(h_2-h_1)x} \\
&\quad + s_\varphi^2 \left(s_\varphi^2 K_{21}e^{i\delta} - c_\varphi^2 K_{12}e^{-i\delta}\right)e^{-i(h_2-h_1)x}\Bigg\}, \\
\Phi_{22} &= K_{22} - 2c_\varphi^2 s_\varphi^2 \left(K_{22} - K_{11}\right) + c_\varphi^2 s_\varphi^2 \left(K_{22} - K_{11}\right)\left\{e^{i(h_2-h_1)x} + e^{-i(h_2-h_1)x}\right\} \\
&\quad + c_\varphi s_\varphi \Bigg[\cos 2\varphi \left(K_{12}e^{-i\delta} + K_{21}e^{i\delta}\right) + \left(s_\varphi^2 K_{12}e^{-i\delta} - c_\varphi^2 K_{21}e^{i\delta}\right)e^{i(h_2-h_1)x} \\
&\quad - \left(c_\varphi^2 K_{12}e^{-i\delta} - s_\varphi^2 K_{21}e^{i\delta}\right)e^{-i(h_2-h_1)x}\Bigg], \\
\Phi_{23} &= e^{-i\delta}\Bigg[\left(c_\varphi s_\varphi K_{13} + c_\varphi^2 K_{23}e^{i\delta}\right)e^{-i(h_3-h_2)x} - \left(c_\varphi s_\varphi K_{13} - s_\varphi^2 K_{23}e^{i\delta}\right)e^{-i(h_3-h_1)x}\Bigg],
\end{aligned}$$

$$\begin{aligned}
\Phi_{31} &= \left(s_\varphi^2 K_{31} + c_\varphi s_\varphi K_{32}e^{-i\delta}\right)e^{i(h_3-h_2)x} + \left(c_\varphi^2 K_{31} - c_\varphi s_\varphi K_{32}e^{-i\delta}\right)e^{i(h_3-h_1)x}, \\
\Phi_{32} &= e^{i\delta}\Bigg[\left(c_\varphi s_\varphi K_{31} + c_\varphi^2 K_{32}e^{-i\delta}\right)e^{i(h_3-h_2)x} - \left(c_\varphi s_\varphi K_{31} - s_\varphi^2 K_{32}e^{-i\delta}\right)e^{i(h_3-h_1)x}\Bigg], \\
\Phi_{33} &= K_{33}.
\end{aligned} \tag{A3}$$

Appendix B. The first-order tilde-basis unitary evolution $\widetilde{S}$ matrix elements

Here, we present the result of unitary $\widetilde{S}$ matrix elements which come from the first-order UV parameter related part of the Hamiltonian.

$$\begin{aligned}
&\widetilde{S}(x)^{\mathrm{EV}}_{11} \\
&= \Delta_b \left\{K_{11} + 2c_\varphi^2 s_\varphi^2 \left(K_{22} - K_{11}\right) - c_\varphi s_\varphi \cos 2\varphi \left(K_{12}e^{-i\delta} + K_{21}e^{i\delta}\right)\right\}(-ix)\left(c_\varphi^2 e^{-ih_1 x} + s_\varphi^2 e^{-ih_2 x}\right) \\
&+ c_\varphi s_\varphi \left\{c_\varphi s_\varphi \cos 2\varphi \left(K_{22} - K_{11}\right) + 2c_\varphi^2 s_\varphi^2 \left(K_{12}e^{-i\delta} + K_{21}e^{i\delta}\right)\right\}(-ix)\left(e^{-ih_2 x} - e^{-ih_1 x}\right)
\end{aligned}$$

$$+ c_\varphi s_\varphi \left[-2c_\varphi s_\varphi \left(K_{22}-K_{11}\right) + \cos 2\varphi \left(K_{12}e^{-i\delta}+K_{21}e^{i\delta}\right)\right] \frac{1}{h_2-h_1}\left(e^{-ih_2x}-e^{-ih_1x}\right). \tag{B1}$$

$$\begin{aligned}
&\widetilde{S}(x)^{\mathrm{EV}}_{12} \\
&= e^{i\delta}\Delta_b\Bigg[\left\{c_\varphi s_\varphi \cos 2\varphi \left(K_{22}-K_{11}\right) + 2c_\varphi^2 s_\varphi^2 \left(K_{12}e^{-i\delta}+K_{21}e^{i\delta}\right)\right\}(-ix)\left(c_\varphi^2 e^{-ih_1x}+s_\varphi^2 e^{-ih_2x}\right) \\
&+ c_\varphi s_\varphi \left\{K_{22}-2c_\varphi^2 s_\varphi^2 \left(K_{22}-K_{11}\right) + c_\varphi s_\varphi \cos 2\varphi \left(K_{12}e^{-i\delta}+K_{21}e^{i\delta}\right)\right\}(-ix)\left(e^{-ih_2x}-e^{-ih_1x}\right) \\
&+ \left\{-c_\varphi s_\varphi \cos 2\varphi \left(K_{22}-K_{11}\right) + \left\{K_{12}e^{-i\delta}-2c_\varphi^2 s_\varphi^2 \left(K_{12}e^{-i\delta}+K_{21}e^{i\delta}\right)\right\}\right\}\frac{1}{h_2-h_1}\left(e^{-ih_2x}-e^{-ih_1x}\right)\Bigg].
\end{aligned} \tag{B2}$$

$$\begin{aligned}
\widetilde{S}(x)^{\mathrm{EV}}_{13} = \Delta_b\Bigg[&\left(s_\varphi^2 K_{13} + c_\varphi s_\varphi K_{23}e^{i\delta}\right)\frac{1}{h_3-h_2}\left(e^{-ih_3x}-e^{-ih_2x}\right) \\
&+ \left(c_\varphi^2 K_{13} - c_\varphi s_\varphi K_{23}e^{i\delta}\right)\frac{1}{h_3-h_1}\left(e^{-ih_3x}-e^{-ih_1x}\right)\Bigg].
\end{aligned} \tag{B3}$$

$$\begin{aligned}
&\widetilde{S}(x)^{\mathrm{EV}}_{21} \\
&= e^{-i\delta}\Delta_b\Bigg[\left\{c_\varphi s_\varphi \cos 2\varphi \left(K_{22}-K_{11}\right) + 2c_\varphi^2 s_\varphi^2 \left(K_{12}e^{-i\delta}+K_{21}e^{i\delta}\right)\right\}(-ix)\left(s_\varphi^2 e^{-ih_1x}+c_\varphi^2 e^{-ih_2x}\right) \\
&+ c_\varphi s_\varphi \left\{K_{11}+2c_\varphi^2 s_\varphi^2 \left(K_{22}-K_{11}\right) - c_\varphi s_\varphi \cos 2\varphi \left(K_{12}e^{-i\delta}+K_{21}e^{i\delta}\right)\right\}(-ix)\left(e^{-ih_2x}-e^{-ih_1x}\right) \\
&+ \left\{-c_\varphi s_\varphi \cos 2\varphi \left(K_{22}-K_{11}\right) + \left\{K_{21}e^{i\delta}-2c_\varphi^2 s_\varphi^2 \left(K_{12}e^{-i\delta}+K_{21}e^{i\delta}\right)\right\}\right\}\frac{1}{h_2-h_1}\left(e^{-ih_2x}-e^{-ih_1x}\right)\Bigg].
\end{aligned} \tag{B4}$$

$$\begin{aligned}
&\widetilde{S}(x)^{\mathrm{EV}}_{22} \\
&= \Delta_b\Bigg[c_\varphi s_\varphi \left\{c_\varphi s_\varphi \cos 2\varphi \left(K_{22}-K_{11}\right) + 2c_\varphi^2 s_\varphi^2 \left(K_{12}e^{-i\delta}+K_{21}e^{i\delta}\right)\right\}(-ix)\left(e^{-ih_2x}-e^{-ih_1x}\right) \\
&+ \left\{K_{22}-2c_\varphi^2 s_\varphi^2 \left(K_{22}-K_{11}\right) + c_\varphi s_\varphi \cos 2\varphi \left(K_{12}e^{-i\delta}+K_{21}e^{i\delta}\right)\right\}(-ix)\left(s_\varphi^2 e^{-ih_1x}+c_\varphi^2 e^{-ih_2x}\right) \\
&+ \left\{2c_\varphi^2 s_\varphi^2 \left(K_{22}-K_{11}\right) - c_\varphi s_\varphi \cos 2\varphi \left(K_{12}e^{-i\delta}+K_{21}e^{i\delta}\right)\right\}\frac{1}{h_2-h_1}\left(e^{-ih_2x}-e^{-ih_1x}\right)\Bigg].
\end{aligned} \tag{B5}$$

$$\begin{aligned}
\widetilde{S}(x)^{\mathrm{EV}}_{23} = e^{-i\delta}\Delta_b\Bigg\{&\left[c_\varphi s_\varphi K_{13} + c_\varphi^2 K_{23}e^{i\delta}\right]\frac{1}{h_3-h_2}\left(e^{-ih_3x}-e^{-ih_2x}\right) \\
&- \left[c_\varphi s_\varphi K_{13} - s_\varphi^2 K_{23}e^{i\delta}\right]\frac{1}{h_3-h_1}\left(e^{-ih_3x}-e^{-ih_1x}\right)\Bigg\}.
\end{aligned} \tag{B6}$$

$$\widetilde{S}(x)^{\mathrm{EV}}_{31} = \Delta_b\Bigg[\left(s_\varphi^2 K_{31} + c_\varphi s_\varphi K_{32}e^{-i\delta}\right)\frac{1}{h_3-h_2}\left(e^{-ih_3x}-e^{-ih_2x}\right)$$

$$+\left(c_\varphi^2 K_{31} - c_\varphi s_\varphi K_{32} e^{-i\delta}\right)\frac{1}{h_3 - h_1}\left(e^{-ih_3 x} - e^{-ih_1 x}\right)\Bigg]. \tag{B7}$$

$$\widetilde{S}(x)^{\rm EV}_{32} = e^{i\delta}\Delta_b\Bigg[\left(c_\varphi s_\varphi K_{31} + c_\varphi^2 K_{32} e^{-i\delta}\right)\frac{1}{h_3 - h_2}\left\{e^{-ih_3 x} - e^{-ih_2 x}\right\}$$
$$-\left(c_\varphi s_\varphi K_{31} - s_\varphi^2 K_{32} e^{-i\delta}\right)\frac{1}{h_3 - h_1}\left\{e^{-ih_3 x} - e^{-ih_1 x}\right\}\Bigg]. \tag{B8}$$

$$\widetilde{S}(x)^{\rm EV}_{33} = (-ix\Delta_b)\, e^{-ih_3 x} K_{33}. \tag{B9}$$

Appendix C. The zeroth-order νSM S matrix elements

Here, we give the expressions of the flavor-basis S matrix elements of νSM part at zeroth order. The superscript "νSM" is abbreviated.

$$\begin{aligned}
S^{(0)}_{ee} &= c_{13}^2\left(c_\varphi^2 e^{-ih_1 x} + s_\varphi^2 e^{-ih_2 x}\right) + s_{13}^2 e^{-ih_3 x},\\
S^{(0)}_{e\mu} &= c_{23}c_{13}c_\varphi s_\varphi e^{i\delta}\left(e^{-ih_2 x} - e^{-ih_1 x}\right) - s_{23}c_{13}s_{13}\left(c_\varphi^2 e^{-ih_1 x} + s_\varphi^2 e^{-ih_2 x} - e^{-ih_3 x}\right),\\
S^{(0)}_{e\tau} &= -c_{23}c_{13}s_{13}\left(c_\varphi^2 e^{-ih_1 x} + s_\varphi^2 e^{-ih_2 x} - e^{-ih_3 x}\right) - s_{23}c_{13}c_\varphi s_\varphi e^{i\delta}\left(e^{-ih_2 x} - e^{-ih_1 x}\right),\\
S^{(0)}_{\mu e} &= c_{23}c_{13}c_\varphi s_\varphi e^{-i\delta}\left(e^{-ih_2 x} - e^{-ih_1 x}\right) - s_{23}c_{13}s_{13}\left(c_\varphi^2 e^{-ih_1 x} + s_\varphi^2 e^{-ih_2 x} - e^{-ih_3 x}\right) = S_{e\mu}(-\delta),\\
S^{(0)}_{\mu\mu} &= c_{23}^2\left(s_\varphi^2 e^{-ih_1 x} + c_\varphi^2 e^{-ih_2 x}\right) + s_{23}^2\left\{s_{13}^2\left(c_\varphi^2 e^{-ih_1 x} + s_\varphi^2 e^{-ih_2 x}\right) + c_{13}^2 e^{-ih_3 x}\right\}\\
&\quad - 2c_{23}s_{23}s_{13}c_\varphi s_\varphi\cos\delta\left(e^{-ih_2 x} - e^{-ih_1 x}\right),\\
S^{(0)}_{\mu\tau} &= s_{13}c_\varphi s_\varphi\left(s_{23}^2 e^{i\delta} - c_{23}^2 e^{-i\delta}\right)\left(e^{-ih_2 x} - e^{-ih_1 x}\right)\\
&\quad + c_{23}s_{23}\left[s_{13}^2\left(c_\varphi^2 e^{-ih_1 x} + s_\varphi^2 e^{-ih_2 x}\right) + c_{13}^2 e^{-ih_3 x} - \left(s_\varphi^2 e^{-ih_1 x} + c_\varphi^2 e^{-ih_2 x}\right)\right],\\
S^{(0)}_{\tau e} &= -c_{23}c_{13}s_{13}\left(c_\varphi^2 e^{-ih_1 x} + s_\varphi^2 e^{-ih_2 x} - e^{-ih_3 x}\right) - s_{23}c_{13}c_\varphi s_\varphi e^{-i\delta}\left(e^{-ih_2 x} - e^{-ih_1 x}\right) = S_{e\tau}(-\delta),\\
S^{(0)}_{\tau\mu} &= s_{13}c_\varphi s_\varphi\left(s_{23}^2 e^{-i\delta} - c_{23}^2 e^{i\delta}\right)\left(e^{-ih_2 x} - e^{-ih_1 x}\right)\\
&\quad + c_{23}s_{23}\left[s_{13}^2\left(c_\varphi^2 e^{-ih_1 x} + s_\varphi^2 e^{-ih_2 x}\right) + c_{13}^2 e^{-ih_3 x} - \left(s_\varphi^2 e^{-ih_1 x} + c_\varphi^2 e^{-ih_2 x}\right)\right] = S_{\mu\tau}(-\delta),\\
S^{(0)}_{\tau\tau} &= s_{23}^2\left(s_\varphi^2 e^{-ih_1 x} + c_\varphi^2 e^{-ih_2 x}\right) + c_{23}^2\left\{s_{13}^2\left(c_\varphi^2 e^{-ih_1 x} + s_\varphi^2 e^{-ih_2 x}\right) + c_{13}^2 e^{-ih_3 x}\right\}\\
&\quad + 2c_{23}s_{23}s_{13}c_\varphi s_\varphi\cos\delta\left(e^{-ih_2 x} - e^{-ih_1 x}\right).
\end{aligned} \tag{C1}$$

Appendix D. The neutrino oscillation probability in the $\nu_\mu \to \nu_e$ and the other channels

In this appendix, we give the expressions of the rest of the terms of $P(\nu_\mu \to \nu_e)^{(1)}_{\rm EV}$ which are not presented in Sect. 5. We also briefly mention how to compute the neutrino oscillation probability in the ν_μ–ν_τ sector.

Appendix D.1. The neutrino oscillation probability in the $\nu_\mu \to \nu_e$ channel: The rest of the unitary evolution part

We recapitulate the definition (58) of the four terms of $P(\nu_\mu \to \nu_e)^{(1)}_{\rm EV}$ again for convenience:

$$\begin{aligned} P(\nu_\mu \to \nu_e)^{(1)}_{\rm EV} &= P(\nu_\mu \to \nu_e)^{(1)}_{\rm EV}|_{\rm D\text{-}OD} \\ &+ P(\nu_\mu \to \nu_e)^{(1)}_{\text{int-UV}}|_{\rm OD1} + P(\nu_\mu \to \nu_e)^{(1)}_{\text{int-UV}}|_{\rm OD2} + P(\nu_\mu \to \nu_e)^{(1)}_{\text{int-UV}}|_{\rm OD3}, \end{aligned} \tag{D1}$$

where the subscripts "D" and "OD" refer to the diagonal and the off-diagonal K_{ij} variables.

The first term of Eq. (D1) is given in Eq. (59). Now, we present the remaining three "OD" terms:

$$\begin{aligned} &P(\nu_\mu \to \nu_e)^{(1)}_{\rm EV}|_{\rm OD1} \\ &= 4c_{23}c_{13}^2 {\rm Re}\left(K_{12}e^{-i\delta}\right) \\ &\times \frac{\Delta_b}{h_2-h_1}\left[-s_{23}\cos\delta\left\{\sin^2\frac{(h_3-h_2)x}{2} - \sin^2\frac{(h_3-h_1)x}{2} - \cos 2\varphi \sin^2\frac{(h_2-h_1)x}{2}\right\}\right. \\ &\left. + c_{23}\sin 2\varphi \sin^2\frac{(h_2-h_1)x}{2} + 2s_{23}\sin\delta\sin\frac{(h_3-h_2)x}{2}\sin\frac{(h_2-h_1)x}{2}\sin\frac{(h_1-h_3)x}{2}\right] \\ &+ 4c_{23}s_{23}c_{13}^2 {\rm Im}\left(K_{12}e^{-i\delta}\right) \\ &\times \frac{\Delta_b}{h_2-h_1}\left[\sin\delta\left\{\sin^2\frac{(h_3-h_2)x}{2} - \sin^2\frac{(h_3-h_1)x}{2} - \cos 2\varphi \sin^2\frac{(h_2-h_1)x}{2}\right\}\right. \\ &\left. + 2\cos\delta\sin\frac{(h_3-h_2)x}{2}\sin\frac{(h_2-h_1)x}{2}\sin\frac{(h_1-h_3)x}{2}\right]. \end{aligned} \tag{D2}$$

$$\begin{aligned} &P(\nu_\mu \to \nu_e)^{(1)}_{\rm EV}|_{\rm OD2} \\ &= -4c_{23}^2c_{13}s_{13}c_\varphi s_\varphi {\rm Re}\left(c_\varphi s_\varphi K_{31} + c_\varphi^2 K_{32}e^{-i\delta}\right) \\ &\times \frac{\Delta_b}{h_3-h_2}\left\{\sin^2\frac{(h_3-h_2)x}{2} - \sin^2\frac{(h_3-h_1)x}{2} + \sin^2\frac{(h_2-h_1)x}{2}\right\} \\ &+ 4c_{23}^2c_{13}s_{13}c_\varphi s_\varphi {\rm Re}\left(c_\varphi s_\varphi K_{31} - s_\varphi^2 K_{32}e^{-i\delta}\right) \\ &\times \frac{\Delta_b}{h_3-h_1}\left\{\sin^2\frac{(h_3-h_2)x}{2} - \sin^2\frac{(h_3-h_1)x}{2} - \sin^2\frac{(h_2-h_1)x}{2}\right\} \\ &+ 4c_{23}s_{23}c_{13}s_{13}^2\left\{\cos\delta{\rm Re}\left(c_\varphi s_\varphi K_{31} + c_\varphi^2 K_{32}e^{-i\delta}\right) - \sin\delta{\rm Im}\left(c_\varphi s_\varphi K_{31} + c_\varphi^2 K_{32}e^{-i\delta}\right)\right\} \\ &\times \frac{\Delta_b}{h_3-h_2}\left[c_\varphi^2\left\{\sin^2\frac{(h_3-h_1)x}{2} - \sin^2\frac{(h_2-h_1)x}{2}\right\} + (1+s_\varphi^2)\sin^2\frac{(h_3-h_2)x}{2}\right] \\ &- 4c_{23}s_{23}c_{13}s_{13}^2\left\{\cos\delta{\rm Re}\left(c_\varphi s_\varphi K_{31} - s_\varphi^2 K_{32}e^{-i\delta}\right) - \sin\delta{\rm Im}\left(c_\varphi s_\varphi K_{31} - s_\varphi^2 K_{32}e^{-i\delta}\right)\right\} \\ &\times \frac{\Delta_b}{h_3-h_1}\left[s_\varphi^2\left\{\sin^2\frac{(h_3-h_2)x}{2} - \sin^2\frac{(h_2-h_1)x}{2}\right\} + (1+c_\varphi^2)\sin^2\frac{(h_3-h_1)x}{2}\right] \\ &- 8c_{23}c_{13}s_{13}\left[\left(s_{23}s_{13}c_\varphi^2\cos\delta + c_{23}c_\varphi s_\varphi\right){\rm Im}\left(c_\varphi s_\varphi K_{31} + c_\varphi^2 K_{32}e^{-i\delta}\right)\right. \\ &\left. + s_{23}s_{13}c_\varphi^2\sin\delta{\rm Re}\left(c_\varphi s_\varphi K_{31} + c_\varphi^2 K_{32}e^{-i\delta}\right)\right]\frac{\Delta_b}{h_3-h_2}\sin\frac{(h_3-h_2)x}{2}\sin\frac{(h_2-h_1)x}{2}\sin\frac{(h_1-h_3)x}{2} \end{aligned}$$

$$
\begin{aligned}
&- 8c_{23}c_{13}s_{13}\Big[\left(s_{23}s_{13}s_\varphi^2\cos\delta - c_{23}c_\varphi s_\varphi\right)\mathrm{Im}\left(c_\varphi s_\varphi K_{31} - s_\varphi^2 K_{32}e^{-i\delta}\right)\\
&+ s_{23}s_{13}s_\varphi^2\sin\delta\mathrm{Re}\left(c_\varphi s_\varphi K_{31} - s_\varphi^2 K_{32}e^{-i\delta}\right)\Big]\frac{\Delta_b}{h_3-h_1}\sin\frac{(h_3-h_2)x}{2}\sin\frac{(h_2-h_1)x}{2}\sin\frac{(h_1-h_3)x}{2}.
\end{aligned}
\tag{D3}
$$

$$
\begin{aligned}
&P(\nu_\mu\to\nu_e)^{(1)}_{\mathrm{EV}}|_{\mathrm{OD3}}\\
&= -4c_{23}s_{23}c_{13}c_\varphi s_\varphi\Big\{\cos\delta\mathrm{Re}\left[s_\varphi^2\left(c_{13}^2K_{13}-s_{13}^2K_{31}\right)+c_\varphi s_\varphi\left(c_{13}^2K_{23}e^{i\delta}-s_{13}^2K_{32}e^{-i\delta}\right)\right]\\
&+\sin\delta\mathrm{Im}\left[s_\varphi^2\left(c_{13}^2K_{13}-s_{13}^2K_{31}\right)+c_\varphi s_\varphi\left(c_{13}^2K_{23}e^{i\delta}-s_{13}^2K_{32}e^{-i\delta}\right)\right]\Big\}\\
&\times\frac{\Delta_b}{h_3-h_2}\left\{\sin^2\frac{(h_3-h_2)x}{2}-\sin^2\frac{(h_3-h_1)x}{2}+\sin^2\frac{(h_2-h_1)x}{2}\right\}\\
&- 4c_{23}s_{23}c_{13}c_\varphi s_\varphi\Big\{\cos\delta\mathrm{Re}\left[c_\varphi^2\left(c_{13}^2K_{13}-s_{13}^2K_{31}\right)-c_\varphi s_\varphi\left(c_{13}^2K_{23}e^{i\delta}-s_{13}^2K_{32}e^{-i\delta}\right)\right]\\
&+\sin\delta\mathrm{Im}\left[c_\varphi^2\left(c_{13}^2K_{13}-s_{13}^2K_{31}\right)-c_\varphi s_\varphi\left(c_{13}^2K_{23}e^{i\delta}-s_{13}^2K_{32}e^{-i\delta}\right)\right]\Big\}\\
&\times\frac{\Delta_b}{h_3-h_1}\left\{\sin^2\frac{(h_3-h_2)x}{2}-\sin^2\frac{(h_3-h_1)x}{2}-\sin^2\frac{(h_2-h_1)x}{2}\right\}\\
&- 4s_{23}^2c_{13}s_{13}\mathrm{Re}\left[s_\varphi^2\left(c_{13}^2K_{13}-s_{13}^2K_{31}\right)+c_\varphi s_\varphi\left(c_{13}^2K_{23}e^{i\delta}-s_{13}^2K_{32}e^{-i\delta}\right)\right]\\
&\times\frac{\Delta_b}{h_3-h_2}\left[c_\varphi^2\left\{-\sin^2\frac{(h_3-h_1)x}{2}+\sin^2\frac{(h_2-h_1)x}{2}\right\}-(1+s_\varphi^2)\sin^2\frac{(h_3-h_2)x}{2}\right]\\
&- 4s_{23}^2c_{13}s_{13}\mathrm{Re}\left[c_\varphi^2\left(c_{13}^2K_{13}-s_{13}^2K_{31}\right)-c_\varphi s_\varphi\left(c_{13}^2K_{23}e^{i\delta}-s_{13}^2K_{32}e^{-i\delta}\right)\right]\\
&\times\frac{\Delta_b}{h_3-h_1}\left[s_\varphi^2\left\{-\sin^2\frac{(h_3-h_2)x}{2}+\sin^2\frac{(h_2-h_1)x}{2}\right\}-(1+c_\varphi^2)\sin^2\frac{(h_3-h_1)x}{2}\right]\\
&+ 8s_{23}c_{13}\Big\{\left(c_{23}c_\varphi s_\varphi\cos\delta - s_{23}s_{13}c_\varphi^2\right)\mathrm{Im}\left[s_\varphi^2\left(c_{13}^2K_{13}-s_{13}^2K_{31}\right)+c_\varphi s_\varphi\left(c_{13}^2K_{23}e^{i\delta}-s_{13}^2K_{32}e^{-i\delta}\right)\right]\\
&+ c_{23}c_\varphi s_\varphi\sin\delta\mathrm{Re}\left[s_\varphi^2\left(c_{13}^2K_{13}-s_{13}^2K_{31}\right)+c_\varphi s_\varphi\left(c_{13}^2K_{23}e^{i\delta}-s_{13}^2K_{32}e^{-i\delta}\right)\right]\Big\}\\
&\times\frac{\Delta_b}{h_3-h_2}\sin\frac{(h_3-h_2)x}{2}\sin\frac{(h_2-h_1)x}{2}\sin\frac{(h_1-h_3)x}{2}\\
&+ 8s_{23}c_{13}\Big\{\left(c_{23}c_\varphi s_\varphi\cos\delta + s_{23}s_{13}s_\varphi^2\right)\mathrm{Im}\left[c_\varphi^2\left(c_{13}^2K_{13}-s_{13}^2K_{31}\right)-c_\varphi s_\varphi\left(c_{13}^2K_{23}e^{i\delta}-s_{13}^2K_{32}e^{-i\delta}\right)\right]\\
&+ c_{23}c_\varphi s_\varphi\sin\delta\mathrm{Re}\left[c_\varphi^2\left(c_{13}^2K_{13}-s_{13}^2K_{31}\right)-c_\varphi s_\varphi\left(c_{13}^2K_{23}e^{i\delta}-s_{13}^2K_{32}e^{-i\delta}\right)\right]\Big\}\\
&\times\frac{\Delta_b}{h_3-h_1}\sin\frac{(h_3-h_2)x}{2}\sin\frac{(h_2-h_1)x}{2}\sin\frac{(h_1-h_3)x}{2}.
\end{aligned}
\tag{D4}
$$

Appendix D.2. The neutrino oscillation probability in the ν_μ–ν_τ sector

We refrain from explicit computation of the oscillation probabilities in the ν_μ–ν_τ sector. The reason is that the expression is too lengthy and not particularly structure-revealing beyond that which we

have discussed in this paper with the explicit expressions of $P(\nu_\mu \to \nu_e)^{(1)}$. If one still needs these expressions of the probabilities, one can readily calculate them following the instruction given in Sect. 5. For general readers, we recommend to use e.g. mathematica software to perform computation of the oscillation probability using (56) due to its complexity even at first order. Also, we note again that the exact formula [25] exists to fulfill the needs of accurate numerical computation.

References

[1] T. Kajita, Rev. Mod. Phys. **88** 030501 (2016).
[2] A. B. McDonald, Rev. Mod. Phys. **88**, 030502 (2016).
[3] Z. Maki, M. Nakagawa, and S. Sakata, Prog. Theor. Phys. **28**, 870 (1962).
[4] K. Abe et al. [Hyper-Kamiokande Collaboration], arXiv:1805.04163 [physics.ins-det] [Search INSPIRE].
[5] B. Abi et al. [DUNE Collaboration], arXiv:2002.03005 [hep-ex] [Search INSPIRE].
[6] M. Kobayashi and T. Maskawa, Prog. Theor. Phys. **49**, 652 (1973).
[7] J. H. Christenson, J. W. Cronin, V. L. Fitch, and R. Turlay, Phys. Rev. Lett. **13**, 138 (1964).
[8] L. Wolfenstein, Phys. Rev. D **17**, 2369 (1978).
[9] S. P. Mikheyev and A. Y. Smirnov, Sov. J. Nucl. Phys. **42**, 913 (1985) [Yad. Fiz. **42**, 1441 (1985)].
[10] K. Abe et al. [Super-Kamiokande Collaboration], Phys. Rev. D **97**, 072001 (2018) [arXiv:1710.09126 [hep-ex]] [Search INSPIRE].
[11] K. Abe et al. [T2K Collaboration], Nature **580**, 339 (2020); **583**, E16 (2020) [erratum] [arXiv:1910.03887 [hep-ex]] [Search INSPIRE].
[12] M. A. Acero et al. [NOvA Collaboration], Phys. Rev. Lett. **123**, 151803 (2019) [arXiv:1906.04907 [hep-ex]] [Search INSPIRE].
[13] E. Baussan et al. [ESSnuSB Collaboration], Nucl. Phys. B **885**, 127 (2014) [arXiv:1309.7022 [hep-ex]] [Search INSPIRE].
[14] F. An et al. [JUNO Collaboration], J. Phys. G: Nucl. Part. Phys. **43**, 030401 (2016) [arXiv:1507.05613 [physics.ins-det]] [Search INSPIRE].
[15] K. Abe et al. [Hyper-Kamiokande proto- Collaboration], PTEP **2018**, 063C01 (2018) [arXiv:1611.06118 [hep-ex]] [Search INSPIRE].
[16] T. Kajita, H. Minakata, S. Nakayama, and H. Nunokawa, Phys. Rev. D **75**, 013006 (2007) [arXiv:hep-ph/0609286] [Search INSPIRE].
[17] A. Kumar et al. [ICAL Collaboration], Pramana **88**, 79 (2017) [arXiv:1505.07380 [physics.ins-det]] [Search INSPIRE].
[18] M. G. Aartsen et al. [IceCube-Gen2 Collaboration], J. Phys. G **44**, 054006 (2017) [arXiv:1607.02671 [hep-ex]] [Search INSPIRE].
[19] S. Adrián-Martínez et al. [KM3NeT collaboration], J. High Energy Phys. **1705**, 008 (2017) [arXiv:1612.05621 [physics.ins-det]] [Search INSPIRE].
[20] A. Diaz, C. A. Argüelles, G. H. Collin, J. M. Conrad, and M. H. Shaevitz, arXiv:1906.00045 [hep-ex] [Search INSPIRE].
[21] Y. Farzan and A. Yu. Smirnov, Phys. Rev. D **65**, 113001 (2002) [arXiv:hep-ph/0201105] [Search INSPIRE].
[22] S. Antusch, C. Biggio, E. Fernández-Martínez, M. B. Gavela, and J. López-Pavón, J. High Energy Phys. **0610**, 084 (2006) [arXiv:hep-ph/0607020] [Search INSPIRE].
[23] F. J. Escrihuela, D. V. Forero, O. G. Miranda, M. Tórtola, and J. W. F. Valle, Phys. Rev. D **92**, 053009 (2015); **93**, 119905 (2016) [erratum] [arXiv:1503.08879 [hep-ph]] [Search INSPIRE].
[24] C. S. Fong, H. Minakata, and H. Nunokawa, J. High Energy Phys. **1702**, 114 (2017) [arXiv:1609.08623 [hep-ph]] [Search INSPIRE].
[25] C. S. Fong, H. Minakata, and H. Nunokawa, J. High Energy Phys. **1902**, 015 (2019) [arXiv:1712.02798 [hep-ph]] [Search INSPIRE].
[26] M. Blennow, P. Coloma, E. Fernandez-Martinez, J. Hernandez-Garcia, and J. Lopez-Pavon, J. High Energy Phys. **1704**, 153 (2017) [arXiv:1609.08637 [hep-ph]] [Search INSPIRE].
[27] E. Fernández-Martínez, M. B. Gavela, J. López-Pavón, and O. Yasuda, Phys. Lett. B **649**, 427 (2007) [arXiv:hep-ph/0703098] [Search INSPIRE].

[28] S. Goswami and T. Ota, Phys. Rev. D **78**, 033012 (2008) [arXiv:0802.1434 [hep-ph]] [Search INSPIRE].
[29] S. Antusch, M. Blennow, E. Fernandez-Martinez, and J. López-Pavón, Phys. Rev. D **80**, 033002 (2009) [arXiv:0903.3986 [hep-ph]] [Search INSPIRE].
[30] S. Antusch, S. Blanchet, M. Blennow, and E. Fernandez-Martinez, J. High Energy Phys. **1001**, 017 (2010) [arXiv:0910.5957 [hep-ph]] [Search INSPIRE].
[31] S. Antusch and O. Fischer, J. High Energy Phys. **1410**, 094 (2014) [arXiv:1407.6607 [hep-ph]] [Search INSPIRE].
[32] S.-F. Ge, P. Pasquini, M. Tórtola, and J. W. F. Valle, Phys. Rev. D **95**, 033005 (2017) [arXiv:1605.01670 [hep-ph]] [Search INSPIRE].
[33] E. Fernandez-Martinez, J. Hernandez-Garcia, and J. Lopez-Pavon, J. High Energy Phys. **1608**, 033 (2016) [arXiv:1605.08774 [hep-ph]] [Search INSPIRE].
[34] D. Dutta and P. Ghoshal, J. High Energy Phys. **1609**, 110 (2016) [arXiv:1607.02500 [hep-ph]] [Search INSPIRE].
[35] F. J. Escrihuela, D. V. Forero, O. G. Miranda, M. Tórtola, and J. W. F. Valle, New J. Phys. **19**, 093005 (2017) [arXiv:1612.07377 [hep-ph]] [Search INSPIRE].
[36] S. Parke and M. Ross-Lonergan, Phys. Rev. D **93**, 113009 (2016) [arXiv:1508.05095 [hep-ph]] [Search INSPIRE].
[37] K. Kimura, A. Takamura, and H. Yokomakura, Phys. Rev. D **66**, 073005 (2002) [arXiv:hep-ph/0205295] [Search INSPIRE].
[38] I. Martinez-Soler, and H. Minakata, Prog. Theor. Exp. Phys. **2020**, 063B01 (2020) [arXiv:1806.10152 [hep-ph]] [Search INSPIRE].
[39] M. Tanabashi et al. [Particle Data Group], Phys. Rev. D **98**, 030001 (2018).
[40] H. Minakata and S. J. Parke, J. High Energy Phys. **1601**, 180 (2016) [arXiv:1505.01826 [hep-ph]] [Search INSPIRE].
[41] I. Martinez-Soler and H. Minakata, Prog. Theor. Exp. Phys. **2019**, 073B07 (2019) [arXiv:1904.07853 [hep-ph]] [Search INSPIRE].
[42] H. Minakata, I. Martinez-Soler, and K. Okumura, PoS **NuFact2019**, 035 (2019) [arXiv:1911.10057 [hep-ph]] [Search INSPIRE].
[43] O. L. G. Peres and A. Yu. Smirnov, Nucl. Phys. B **680**, 479 (2004) [arXiv:hep-ph/0309312] [Search INSPIRE].
[44] O. L. G. Peres and A. Yu. Smirnov, Phys. Rev. D **79**, 113002 (2009) [arXiv:0903.5323 [hep-ph]] [Search INSPIRE].
[45] E. Kh. Akhmedov, M. Maltoni, and A. Yu. Smirnov, J. High Energy Phys. **0806**, 072 (2008) [arXiv:0804.1466 [hep-ph]] [Search INSPIRE].
[46] S. Razzaque and A. Yu. Smirnov, J. High Energy Phys. **1505**, 139 (2015) [arXiv:1406.1407 [hep-ph]] [Search INSPIRE].
[47] G. Settanta, S. M. Mari, C. Martellini, and P. Montini [JUNO Collaboration], arXiv:1910.11172 [hep-ex] [Search INSPIRE].
[48] K. J. Kelly, P. A. N. Machado, I. Martinez-Soler, S. J. Parke, and Y. F. Perez-Gonzalez, Phys. Rev. Lett. **123**, 081801 (2019) [arXiv:1904.02751 [hep-ph]] [Search INSPIRE].
[49] K. Abe et al. [Hyper-Kamiokande Proto-Collaboration], Prog. Theor. Exp. Phys. **2015**, 053C02 (2015) [arXiv:1502.05199 [hep-ex]] [Search INSPIRE].
[50] T. Ohlsson, Rept. Prog. Phys. **76**, 044201 (2013) [arXiv:1209.2710 [hep-ph]] [Search INSPIRE].
[51] O. G. Miranda and H. Nunokawa, New J. Phys. **17**, 095002 (2015) [arXiv:1505.06254 [hep-ph]] [Search INSPIRE].
[52] Y. Farzan and M. Tórtola, Front. Phys. **6**, 10 (2018) [arXiv:1710.09360 [hep-ph]] [Search INSPIRE].
[53] A. Friedland, C. Lunardini, and M. Maltoni, Phys. Rev. D **70**, 111301(R) (2004) [arXiv:hep-ph/0408264] [Search INSPIRE].
[54] A. Friedland and C. Lunardini, Phys. Rev. D **72**, 053009 (2005) [arXiv:hep-ph/0506143] [Search INSPIRE].
[55] T. Kikuchi, H. Minakata, and S. Uchinami, J. High Energy Phys. **0903**, 114 (2009) [arXiv:0809.3312 [hep-ph]] [Search INSPIRE].
[56] A. Cervera, A. Donini, M. B. Gavela, J. J. Gomez Cádenas, P. Hernández, O. Mena, and S. Rigolin, Nucl. Phys. B **579**, 17 (2000); **593**, 731 (2001) [erratum] [hep-ph/0002108] [Search INSPIRE].

[57] J. Burguet-Castell, M. B. Gavela, J. J. Gómez-Cadenas, P. Hernández, and O. Mena, Nucl. Phys. B **608**, 301 (2001) [arXiv:hep-ph/0103258] [Search INSPIRE].
[58] V. Barger, D. Marfatia, and K. Whisnant, Phys. Rev. D **65**, 073023 (2002) [arXiv:hep-ph/0112119] [Search INSPIRE].
[59] H. Minakata, H. Nunokawa, and S. Parke, Phys. Rev. D **66**, 093012 (2002) [arXiv:hep-ph/0208163] [Search INSPIRE].
[60] P. Huber, T. Schwetz, and J. W. F. Valle, Phys. Rev. D **66**, 013006 (2002) [arXiv:hep-ph/0202048] [Search INSPIRE].
[61] D. Adey et al. [Daya Bay Collaboration], Phys. Rev. Lett. **121**, 241805 (2018) [arXiv:1809.02261 [hep-ex]] [Search INSPIRE].
[62] H. Minakata, Acta Phys. Polon. B **40**, 3023 (2009) [arXiv:0910.5545 [hep-ph]] [Search INSPIRE].
[63] K. Asano and H. Minakata, J. High Energy Phys. **1106**, 022 (2011) [arXiv:1103.4387 [hep-ph]] [Search INSPIRE].
[64] M. C. Gonzalez-Garcia, Y. Grossman, A. Gusso, and Y. Nir, Phys. Rev. D **64**, 096006 (2001) [arXiv:hep-ph/0105159] [Search INSPIRE].
[65] C. Jarlskog, Phys. Rev. Lett. **55**, 1039 (1985); **58**, 1698 (1987) [erratum].
[66] P. B. Denton, H. Minakata, and S. J. Parke, J. High Energy Phys. **1606**, 051 (2016) [arXiv:1604.08167 [hep-ph]] [Search INSPIRE].
[67] M. Ishitsuka, T. Kajita, H. Minakata, and H. Nunokawa, Phys. Rev. D **72**, 033003 (2005) [arXiv:hep-ph/0504026] [Search INSPIRE].